

# Using Deep Learning Models for Standardised Assessments of Urban Ecosystem Services

Joseph Anderson

A thesis submitted for the Joint programme of  
Master's in urban Climate & Sustainability

August 2023



<b>Author</b> Anderson, Joseph	<b>Publication type</b> Thesis	<b>Completion year</b> 2023
<b>Number of pages:</b> 79		
<b>Supervisor I</b> Dr. Henning Günther	<b>Supervisor II</b> Dr. Benjamin Fisher	
<b>Title</b> Using Deep Learning Models for Standardised Assessment of Urban Ecosystem Services		
<b>Degree:</b> Master's in urban Climate & Sustainability		
<b>Abstract</b> (400-500 words)  <p>The benefits that humans receive from their environment, commonly classified as ecosystem services (ES), has a high demand in cities due to the increased population density. As the urban footprint escalates with human population growth, urban ecosystem services (UES) must be considered in urban planning and policymaking.</p> <p>This study seeks to establish a replicable methodology for assessing UES across multiple cities, in order to establish standardised metrics and comparative analyses. Current research trends focus primarily on case studies that are contextualized to the given city, limiting the research's applicability in cross-city comparisons or in developing state or federal policy (García-Pardo et al., 2022). The MAES 4th Report published by the EU JRC (Maes et al., 2016) was used as an international standard for categorizing UES and their associated service providing units. Furthermore, AI and deep learning models are investigated as a tool for efficient and accurate landcover assessments in the urban environment.</p> <p>Applicationa and limitations of ES matrices are highlighted. An alternative approach to ES matrices is proposed, using the MAES 4th report UES providing units and the landcover classifications of the Esri "High Resolution Land Cover Classification – USA" deep learning model. This standardises "Traffic Light" UES matrix is then combined with the outputs of the deep learning model to estimate the relative presence of five regulating UES across ten US cities. Average accuracy per landcover type and per city were calculated, and F1 scores were used for statistical analysis.</p> <p>The initial results of the study are promising, with the adjusted data achieving an average of 89% accuracy per city. In terms of landcover type accuracy, the average for the adjusted data was 88% with F1 scores ranging from .82-.94. calculations for average UES values for the ten cities were also calculated, with notable differences in values between temperate and arid cities.</p> <p>Applications for the methodology are discussed, especially its usability for urban planners and as a standardised UES assessment for comparative research. Limitations and areas of high error are discussed, including "Wetland" and "Barren" landcover classifications, edge effects in the outer extents of study areas, and limitations in current remote sensing capabilities.</p> <p>Finally, future research possibilities are listed that could lead to improved accuracy and utility of the method. This study proposes a replicable remote-sensing based UES assessment methodology that is simple enough for cities with limited resources to replicate, and standardised enough that results can be compared across cities to broaden the comparative research within the field of UES.</p>		
<b>Keywords</b>  Urban Planning, Ecosystem Services, Remote Sensing		
<b>Originality statement.</b> I hereby declare that this Master's dissertation is my own original work, does not contain other people's work without this being stated, cited and referenced, has not been submitted elsewhere in fulfilment of the requirements of this or any other award.		<b>Signature</b>



# TABLE OF CONTENTS

Acknowledgements .....	3
List of figures .....	5
Chapter 1: Introduction .....	7
1.1. Background .....	7
1.2. Aims, Objectives, and Rationale .....	8
1.3. Methods and Results Summary .....	9
Chapter 2: Literature review .....	11
2.1. Green Infrastructure and Ecosystem Services .....	11
2.2. Quantification of Ecosystem Services .....	12
2.2.1. Challenges with Ecosystem Service Matrices .....	14
2.2.2. The MAES 4 <sup>th</sup> Report .....	14
2.3. Ecosystem Service Mapping and Data Assessment .....	17
2.4. Deep Learning, Artificial Intelligence, and Advances in Analytics .....	18
2.5. Literature Review Synthesis and Gap Statement .....	19
Chapter 3: Methodology .....	21
3.1. Methodological Overview .....	21
3.2. Data Sourcing and Strategy Development .....	21
3.3. “Traffic Light” Ecosystem Service Matrix .....	23
3.4. Geospatial Methods .....	25
3.5. Data Analysis Methods .....	26
Chapter 4: Results & conclusions .....	29
4.1. Raw Data .....	29
4.2. Adjustments to Methodology Based on Raw Data .....	32
4.3. Adjusted Data .....	33
4.4. Urban Ecosystem Service Values for Pilot Cities .....	34

Chapter 5: Discussion .....	37
5.1. Results Summary and Significance .....	37
5.2. Limitations .....	38
5.2.1. Barren Soil .....	38
5.2.2. Wetlands .....	39
5.2.3. Albuquerque – Impacts of Adjusted Data .....	40
5.2.4. “Tree Canopy” vs “Shrubland” .....	42
5.2.5. Shadows – Seattle Skyscrapers .....	43
5.2.6. Temporal and Spatial Resolution Limitations .....	44
5.2.7. Edge Effect and Error .....	45
5.2.8. Variability of Accuracy Between Cities .....	46
5.3. Applications .....	48
5.4. Future Research and Recommendations .....	50
5.4.1. Specific Changes to Methodology .....	50
5.4.2. Broader Research Areas .....	53
5.5. Conclusion .....	54
References .....	57
Appendices .....	63
Appendix A Overall Ecosystem Service Value Maps for Each Pilot City .....	63
Appendix B Ground Truthing Tables and Calculations .....	68

## ACKNOWLEDGMENT

I would like to thank my supervisors, Dr. Günther and Dr. Fisher for their support in the development of my thesis aim and methodology. I would further like to thank Dr. Rohinton Emmanuel for his consistent support throughout the program and deep knowledge base on the topic of urban ecosystem services. I would like to thank Dr. Joachim Maes for taking time out of his busy schedule for an interview to educate me about the research of the European Commission on urban ecosystem services, which became foundational to this study. I would like to thank Osman Rafiq for ensuring that the computer lab at Glasgow Caledonian University was available over the summer, as the processing power of multiple computers was critical in completing all spatial analyses in a timely manner. I would also like to thank all MUrCS staff and the Erasmus Mundus programme as a whole for providing me with the opportunity to complete relevant and important research in the field of urban climate and sustainability. Finally, I would like to thank my family and partner for unwavering emotional support during this research.





## LIST OF FIGURES

### Figures:

Figure 1: Decision tree for comparing ES quantification strategies .....	13
Figure 2: Ecosystem service cascade model .....	13
Figure 3: Summary of the MAES UES classes and service providing units .....	16
Figure 4: Distribution of pixel resolution across 83 studies .....	18
Figure 5: Comparison of the UES providing units and landcover classes.....	22
Figure 6: First iteration of the “Traffic Light” ES matrix.....	24
Figure 7: The Model Builder workflow.....	26
Figure 8: Percent accuracy of landcover classification in raw data .....	29
Figure 9: Per-city pixel accuracy of raw data .....	31
Figure 10: Original and edited “Traffic Light” ecosystem services matrix .....	32
Figure 11: Percent accuracy of landcover pixels of adjusted data .....	33
Figure 12: Per-city pixel accuracy of adjusted data .....	34
Figure 13: Combined ES map for Portland, OR .....	35
Figure 14: Results of successive map generation .....	36
Figure 15: Albuquerque classification map and combined ES maps .....	41
Figure 16: Seattle skyscraper shadows .....	43
Figure 17: Edge effect error in Tacoma, WA .....	45
Figure 18: Edge effect error in Portland, OR .....	45
Figure 19: Denver, CO aerial imagery and classification map .....	47
Figure 20: Seattle maps .....	51

### Tables:

Table 1: Summary table for data.....	23
Table 2: F1 Scores for raw data .....	30



## CHAPTER 1: INTRODUCTION

### 1.1. Background

The impacts of cities and urbanization on the environment have been well researched. Humans invariably shape their environment in response to community needs. Indeed, “Hunter-gatherer societies have probably the least impact on the earth but can still substantially modify it – Australian aborigines, for example, radically altered their continent through the use of fire” (Newman, 2006). Modern cities, on the other hand, have a broader range of impacts on the surrounding ecosystems. Impervious surfaces lead to increased water pollution via stormwater runoff, while simultaneously reducing aquifer recharge (Bolund and Hunhammar, 1999). Worse still, urban sprawl has been identified as the leading driver of desertification in Europe, with potentially irreversible impacts on habitat diversity (Barbero-Sierra, Marques and Ruíz-Pérez, 2013).

Within the field, there appears to be an assumption that urbanization has a categorically negative impact on its surroundings. Some even go as far as to refer to cities as “only parasites in the biosphere” (Bolund & Hunhammar, 1999). Nevertheless, cities provide many necessary benefits which should discourage their wholesale dismissal as a feature of a sustainable future. Müller et al. describes urbanization as “a double-edged sword. On one edge, urbanization destroys and fragments natural ecosystems, introduces non-native species, degrades and alters ecosystem processes, and modifies natural disturbance regimes. On the other edge, urbanization creates social and economic opportunities, centers of art and culture, and truly unique ecological spaces through design” (Müller et al., 2013). Furthermore, urban residents of western countries have a smaller per capita carbon footprint than their rural counterparts, due to reduced transportation emissions and economies of scale in infrastructure (Newman, 2006). Therefore, we must investigate the ways in which the built environment is supported by natural systems as a way to incentivise the inclusion of ecological functions within the urban fabric.

To better understand the interactions between natural systems and the urban environment, urban ecosystem services (UES) has been identified as a useful metric ([www.eea.europa.eu](http://www.eea.europa.eu), 2017). And given the geospatial nature of urban planning, it becomes important to find tools for mapping the distribution of UES throughout a city. Currently, there are many approaches

to this topic (Harrison et al., 2018), and a major shortcoming in the field is that most research is predominantly case studies. As such, methodologies are frequently altered between cities to contextualize for the environment. Although contextualization is useful for more nuanced understanding of the site-specific impacts of UES, this makes it challenging to make comparisons between cities, which limits the development of a standardised approach for federal or international-level mapping and policymaking.

## **1.2. Aim, Objectives, and Rationale**

The aim of this research is to investigate the feasibility of measuring UES through remote sensing, using a methodology that is replicable across multiple cities, standardised so results can be compared between sites, and is efficient enough to be accessible to cities with limited resources. That way, the field of UES can grow based on wider datasets that encompass multiple cities and multiple contexts. The objectives necessary to achieve this aim are as follows:

- Design a remote sensing protocol that can classify urban landcover effectively enough to estimate relative presence of urban ecosystem services
- Optimize this protocol to be easily replicable across a variety of sites
- Test this methodology across multiple pilot cities to assess accuracy and identify shortcomings
- Interpret the experimental results to create recommendations that increase the accessibility and applicability of the methodology to other researchers, geospatial analysts, and urban planners

In order to develop urban planning policy that protects and promotes green, liveable cities with ample UES for urban dwellers, data must be accessible and prepared in a way that is usable to policymakers, not just researchers. Despite abundant geospatial data in the United States (C. Daly et al., 2000), it cannot serve to support sustainable urban development unless there is an accessible methodology for converting raw data into actionable insights. Furthermore, to develop state or federal policy that creates specific, measurable targets for UES, universally applicable metrics are necessary for benchmarking the current status of multiple cities and to create tangible milestones to measure progress. When research on UES is primarily case studies

(García-Pardo et al., 2022), it presents challenges to the adoption of data-driven policymaking. Therefore, the rationale behind this research is to expand the quantification of UES to include simplified metrics that can be used to compare between cities effectively and support top-down policy to ensure all cities include meaningful sources of UES.

### **1.3. Methods and Results Summary**

To achieve this goal, a consistent classification scheme for urban ES had to be identified. The MAES 4th report from the European Commission was identified as it created a consistent relationship between landcovers and UES in ten pilot cities across Europe (Maes et al., 2016). Next, an appropriate Artificial Neural Network (ANN) deep learning model was identified that could successfully identify landcover classes in a manner that was compatible with the MAES approach for UES mapping. These two tools were utilized to process a large amount of free high-resolution spectral data for the United States. The result was the implementation of a deep learning model to process 1m resolution data for ten pilot cities across the Western United States, which could then be converted into ecosystem service maps for five of the MAES regulating UES. This research can act as an extension to the MAES 4th report, expanding the approach to include both European and U.S. pilot cities. A statistical analysis of the deep learning model is also included.

The results of this study can expand the accessibility of UES assessments to a much wider range of cities due to the simplicity and accuracy of the identified methodology. It also allows for cities to compare relative concentrations of UES to better inform state, federal, or international policy. Finally, limitations of this methodology are discussed, with possible solutions and further research themes that could improve the efficacy and impact of this study. Overall, the model had an average accuracy of 89% in identifying landcover classifications on a per-city basis, and Chapter 5 includes many applications of the UES assessment to make this method useful to urban planners, policymakers, and environmental scientists interested in the urban environment.



## CHAPTER 2: Literature Review

### 2.1. Green Infrastructure and Ecosystem Services

Urban green infrastructure (UGI) and the associated Ecosystem services (ES) are tools used to understand the relationship between humankind and the environments in which they inhabit. The European Union defines UGI as “A strategically planned network of natural and semi-natural areas with other environmental features designed and managed to deliver a wide range of ecosystem services” (www.eea.europa.eu, 2017). Ecosystem services, on the other hand, requires more nuance to define. In the broadest context, ecosystem services refer to “benefits that people obtain from ecosystems or their direct and indirect contributions to human well-being” (www.eea.europa.eu, 2017). Therefore, urban ecosystem services (UES) can be seen as the quantifiable benefits that UGI and other urban natural spaces provide to a city and its inhabitants.

UGI benefits the built environment through many different mechanisms. Urban vegetation has been studied to reduce air and noise pollution, flood risk, and water pollution (Bolund & Hunhammar, 1999). European cities with at least 16% tree coverage experienced a 1°C reduction in UHI (Marando et al., 2022). And cities with UGI can also be hotspots of higher vascular plant and bird biodiversity than the surrounding rural environment (Müller et al., 2013).

Categorization and analysis of ES includes a variety of approaches. One standard for the categorization of ecosystem services includes three or four main categories (provisioning, cultural, and regulating/support), each broken down into further categories (Trinder, 2021). Additionally, ES can be analyzed in terms of supply and demand (Trinder, 2021). To really understand the needs of a city in terms of ES, Trinder states that “services are combined to form the ecosystem footprint which is the area needed to generate the ES required by a certain region in a timeframe (2021).” This idea of an ecosystem footprint is especially important in urban environments, where space for natural areas to supply ES can be limited compared to the population and subsequent ES demand. ES is also commonly quantified through cost-benefit analyses, in order to make prudent financial decisions in urban spatial planning (Newman, 2006). Although UGI can improve the urban environment and is sometimes more

affordable than grey infrastructure for the same benefits (Newman, 2006), quantification of ES, particularly in the urban environment, can be difficult.

## **2.2. Quantification of Ecosystem Services**

There are many strategies for the quantification and categorization of ES. One method is the urban vegetation structure types (UVST), which provides an analytical process to “estimate the provision and quality of green space per capita in individual urban districts” (Mathey et al., 2021). The UVST approach has also been used to estimate ES provided by different types of green spaces (Lehmann et al., 2014). UVST has been primarily used to measure microclimatic changes within a city. Provisioning ES (broadly, supplies of water, food, and other resources) can typically be categorized with a land use map, as this kind of ES is typically defined by productive forests, agricultural land, and watershed recharge areas. One study found over 20 categories of ES quantification strategies (Harrison et al., 2018). Due to the wide variety of tools and approaches to ES mapping, there has not yet been any standardised procedure for UES assessments. This presents a challenge to comparative assessments of ES, because each different method has a different output, and as such, results can be challenging to compare between studies.

To determine the best technique for ES quantification for the aim mentioned in Chapter 1, it can be helpful to organize established methods based on the desired outcome and data available. Harrison et al. (2018) developed a decision tree for comparing ES quantification methodologies, with the initial decision being whether method focuses on biophysical, social or economic factors of ES (see figure 1). Because this study focuses on distribution of biophysical characteristics of UES through mapping, a landcover-based matrix was determined to be the ideal technique. Maes et al. argue that the ES cascade model is the ideal for organizing ES mapping for EU-wide reporting (Maes et al., 2012). By linking biodiversity and ecosystems to create a flowchart, the ES cascade model “helps in emphasizing the importance of resilience as ecosystem functions are a crucial step in providing ecosystem services” (Maes et al., 2012). As can be seen in figure 2, different ecosystem structures are assigned functions, which then are translated into ES. From there, benefits and values of ES can be assigned. This method is



also compatible with ES matrices, because the starting point of the cascade model is the ecosystem structures, which can be defined through landcover classes.

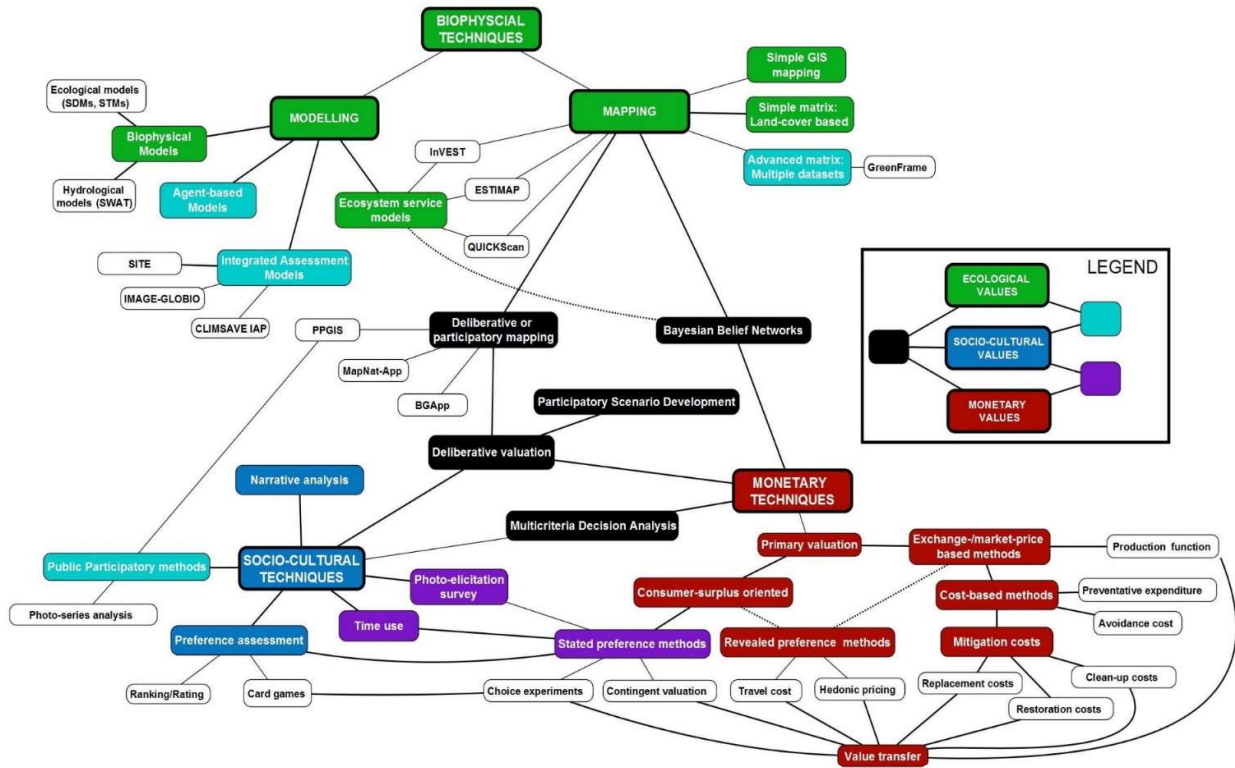


Figure 1: Decision tree for comparing ES quantification strategies (Harrison et al., 2018).

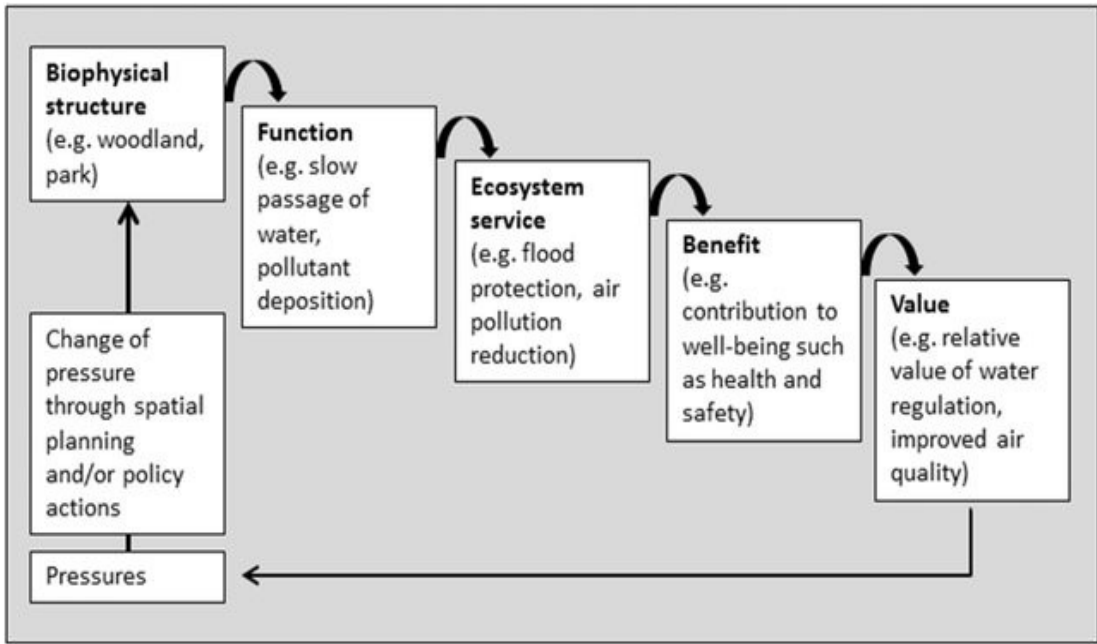


Figure 2: Ecosystem service cascade model (Andersson-Sköld et al., 2018).

### **2.2.1. Challenges with Ecosystem Service Matrices**

ES matrices have become a popular approach to ES quantification over the last ten years, because they allow for the comparison of more types of ES than other methods (Campagne et al., 2020). And understanding multiple ES at once is preferred for land use planning, so that multiple ES can be appropriately considered in land use plans. There have, however, been notable critiques of the ES matrix approach.

According to Luederitz et al., “Urban ecosystem services research needs to be carefully contextualized in relation to the specific locations in which such services arise and are appropriated. Since values ascribed to ecosystem services are not fixed, but vary between urban locations due to contextual features (Ernstson, 2013) cultural identity (Chan et al., 2012) and individual and institutional perceptions (Raymond et al., 2013), the value ascription of relevant (urban) stakeholders in the valuation process is crucial in understanding the actual benefits of urban ecosystem services” (2015). However, a meta-analysis of over 100 studies using ES matrices revealed that 51% of these studies simply copied a ES matrix from another paper, and 27% did not clearly explain the methodology used to assign values within their matrices (Campagne et al., 2020). Herein lies one of the major issues with ES matrices. When the dimensionless unit of “Ecosystem Service Supply” is contextualized to a specific place, it limits its applicability in comparative research. City-specific values of “ES supply” can sometimes make the results more relevant to policymaking in that particular place. However, as variability increases in ES matrices, the dimensionless unit of “ES supply” becomes increasingly vague for researchers. And when the most common mode of contextualization is a panel of local experts (where the decision making process and identities of the experts are often not defined) (Campagne et al., 2020), or matrices are copied from different studies from different contexts, the contextualization process can be a source of increased error and ambiguity in the outcomes. An alternative approach would be to create UES matrices that can function with little or no contextualization, to create a consistent unit for comparative research.

### **2.2.2. The MAES 4<sup>th</sup> Report**

Because ES quantification has relevance on a global level, using an internationally accepted standard of ES, rather than developing a unique framework for this study, is preferred. This is

particularly challenging in the urban environment, since ES research often focuses on broader land management contexts as opposed to the liveability and climate resilience of cities.

The European Commission launched an initiative in 2013 to develop quantitative and consistent approach to ES assessment, entitled, “Mapping and Assessments of Ecosystem Services” (Burkhard and Maes, 2017). In 2016, the 4th report of this initiative was released, which focused specifically on ES in the urban environment (Maes et al., 2016). Using ten pilot cities across Europe, different UES assessments were performed, and then synthesized to develop a more standardised framework. At the time of this writing, this had been the only attempt to develop consistent metrics for UES across an entire continent.

One of the outcomes of the report was a table of key ES, translated for the urban environment, and the landcover types, also known as Service Providing Units, that provide that UES (See figure 3). These UES and the Servicing Providing Units have the potential to be combined for a novel ES matrix that offers consistent categories for urban applications.

CICES Section	CICES Class	Class type (urban ecosystem services)	Service providing unit (SPU)	Demand
Provisioning	Cultivated crops	Vegetables produced by urban allotments and in and the commuting zone	Crop fields, fruit trees, private and public gardens	Consumption
	Surface water for drinking		Watershed	
	Ground water for drinking			
	Surface water for non-drinking purposes			
	Ground water for non-drinking purposes			
Regulating	Filtration/sequestration/storage/accumulation by ecosystems	Regulation of air quality by urban trees and forests	Forest, trees, shrubs	Risk of exposure to pollutant concentration beyond thresholds
	Global climate regulation by reduction of greenhouse gas concentration	Climate regulation by reduction of CO <sub>2</sub>	Vegetation, soil	
	Micro and regional climate regulation	Urban temperature regulation	Forest, trees, shrub, herbs, lawns, wetlands, water bodies	Risk of exposure to high temperatures
	Mediation of smell/noise/visual impacts	Noise mitigated by urban vegetation	Forest, trees, shrubs, vegetated surfaces	Risk of exposure to noise
	Hydrological cycle and water flow maintenance	Water flow regulation and run off mitigation	Trees, shrubs, vegetated and permeable surfaces	Risk for flood sensitive areas or land use
	Flood control		Wetlands	Exposure to flooding
	Pollination and seed dispersal	Insect pollination	Crop fields, fruit trees, private and public gardens	Dependency on insect pollination
Cultural	Physical use of land/seascapes in different environmental	Nature based recreation	Parks, gardens, forest, trees, agricultural areas in the commuting zone,	Preferences; Potential and direct use

Figure 3: Summary of the MAES UES classes and service providing units (Maes et al., 2016)

### 2.3. Ecosystem Service Mapping and Data Assessment

To draw meaningful conclusions regarding the efficacy of a standardised UES mapping approach, results must be generated using data from multiple cities and locations. Fortunately, in recent years there have been major advancements in the use of remotely sensed spectral data in cartography and land use planning. When it comes to ES data, as of 2015 there were 211 separate studies that used remote sensing for ES data collection (de Araujo Barbosa, Caio C, Atkinson, & Dearing, 2015). Even in 2015, the authors believed that “integration of ecosystem services valuation methods and remote sensing observation seems to be the only practical and realistic approaches to regionalise our understanding of complex interdependent socio-ecological systems” (de Araujo Barbosa, Atkinson and Dearing, 2015). García-Pardo et al. claim that “a specific assessment at an urban scale can be generated where remote sensing is really optimised in a cost- and time-efficient way. This is also sustained by the diversity of remote sensing data available that shows the possibility to diagnose and estimate vegetation impacts in the environment without the need for ground-based monitoring, leading to decision making in urban management and planning” (2022).

A meta-analysis in 2022 of 83 studies related to remote sensing and UES found that research was broken into three categories: projects where only passive sensors were used, a combination of passive and active sensors (i.e. LiDAR), and a combination of remotely sensed data with other data sources (i.e. cadastral, weather, social media, ground-based measurements) (García-Pardo et al., 2022). One of the challenges of data from “other data asources” is that it may not be consistent across different cities and regions, whereas remotely sensed data is often formatted similarly across multiple locations. This presents an obstacle for the development of an ES quantification protocol that is applicable to multiple cities if it relies on “other data sources”, because the protocol will have to be adjusted to accommodate how each city formats data. Therefore, the more that a methodology can prioritize remotely-sensed data, the better the results will be for comparative analyses between cities.

These findings are of particular relevance to the U.S., since the U.S. has historically been a leader in remote sensing research and has some of the most robust free databases of remote sensing data (C. Daly et al., 2000). This includes databases for 1m resolution data. As can be seen in figure 4, most research in remote sensing and urban ecosystems is at 30m resolution,

simply because that is the main resolution of free satellite data (García-Pardo et al., 2022). However, given the spatial heterogeneity of the urban environment, that resolution will likely lead to significant error in municipal and neighbourhood-level assessments. With the availability of 1m resolution spectral data, the U.S. has the potential to lead the world in the mapping and monitoring of UES.

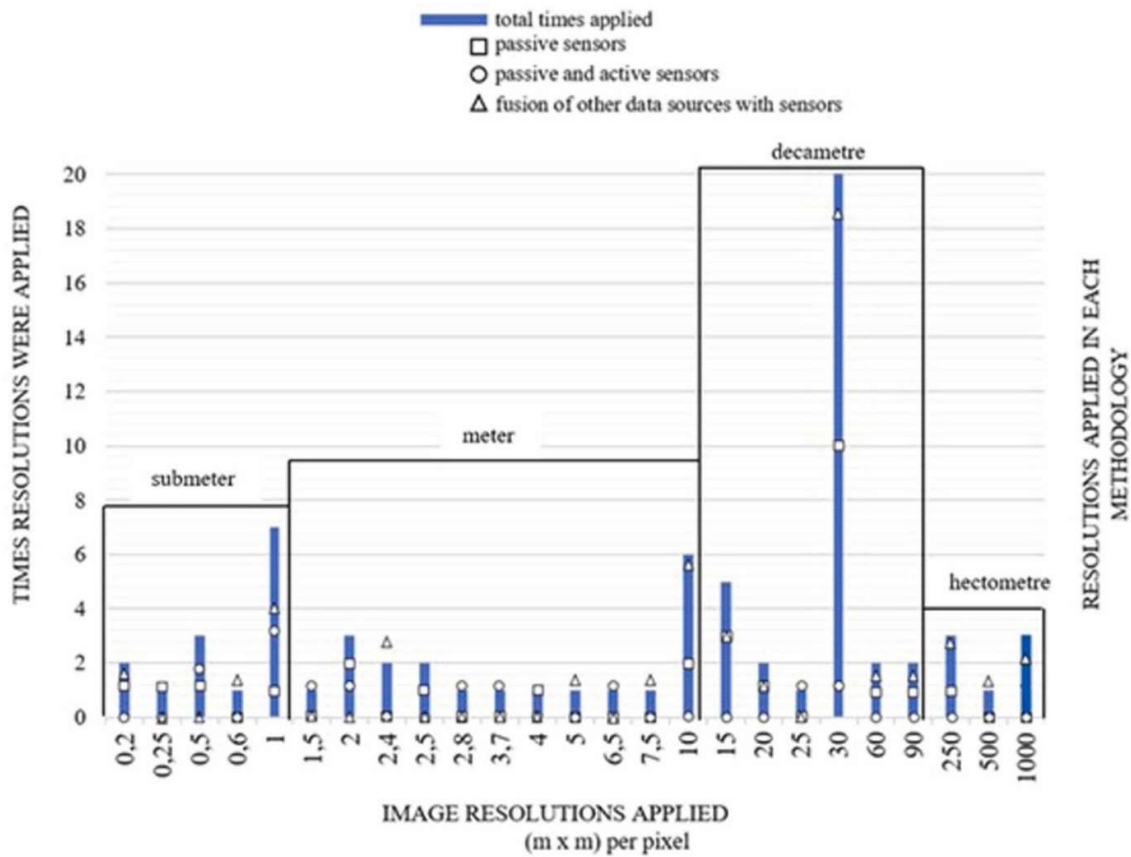


Figure 4: Distribution of pixel resolution across 83 studies focused on remote sensing and UES (García-Pardo et al., 2022).

## 2.4. Deep Learning, Artificial Intelligence, and Advances in Analytics

The high volume of remotely sensed data can be helpful, but one potential barrier of its widespread utilization in UES assessments is the technical skill and time required by a geospatial analyst to generate meaningful conclusions from raw spectral data. Fortunately, advances in artificial intelligence (AI) and deep learning models have begun rapidly shifting the way geospatial and environmental data can be assessed.



Deep learning and certain applications of AI have been integrated with some tools in ArcGIS Pro for some time now. Object-based classification relies on a machine learning to estimate object extent in the disaggregated raw pixel data (Liu and Xia, 2010). However, individual developers are continuing to develop GIS-compatible deep learning models for specific applications. Stanford University's InVEST modelling program, for example, combines remotely sensed and GIS data to elucidate relationships between human behaviour and environmental health for terrestrial and aquatic ecosystems (Hack, Molewijk and Beißler, 2020). The tools in the InVEST model are currently being expanded to work with urban environments (Delpy et al., 2021). One meta-analysis found 140 papers from as early as 1997 through 2016 that used AI to process urban geography data, and found the AI techniques worked better than a conventional approach in 75% of studies (Grekousis, 2019). And at the time of writing, Esri Analytics has 56 deep learning models available on the Living Atlas database, many of which perform different types of object identification and classification on spectral data (Esri, 2023b).

Though these deep learning and AI tools are very useful, widespread implementation in geospatial analysis has been slow compared to other fields (Grekousis, 2019). Because many of these tools are fairly new, there is generally a smaller pool of geospatial analysts who are familiar with and comfortable using these models. Another challenge in the adoption of these tools is that many of them are considered black box technologies (Grekousis, 2019). Researchers sometimes avoid black box tools, because if there are errors or unusual results, it is difficult or even impossible to understand the mechanics which caused the problem, let alone resolve them. Despite these limitations, deep learning and AI have already changed data management in the field of geanalytics and will likely continue to do so.

## **2.5. Literature Review Synthesis and Gap Statement**

Although ES matrices were identified by Harrison et al. as an effective mapping technique for the biophysical components of UES (2018), the challenges outlined in section 2.2.1 indicate that a novel approach to ES matrices are required to be an effective comparative tool for UES across different locations. And with remote sensed data being considered to be the only cost-effective approach for ES assessments (de Araujo Barbosa, Atkinson and Dearing, 2015), and the widely available and relatively consistent nature of remote sensing data (C. Daly et al.,

2000), this novel approach must utilize this resource. This study aims to address this gap in ES matrix research, using standardised data sources and methodologies to increase the availability of comparative and consistent UES assessments using the ES matrix approach.

It is clear that to begin a standardised approach to ES matrices, a large amount of data will be necessary across multiple cities for a broadly applicable methodology, as opposed to isolated case studies. Deep learning models can significantly increase the number of sites analysed by a single geospatial analyst. And the framework for UES assessments provided by the MAES 4th report is a robust and consistent outline for a novel ES matrix. Finally, the data availability in the United States offers a large reservoir for testing of remote sensing-based UES assessments. Therefore, in theory, it should be possible to expand the scope of the MAES UES mapping research to an international context through free U.S. data, and increase the pace and success of this research through the adoption of deep learning models.



## CHAPTER 3: Methodology

### 3.1. Methodological Overview

In the development of the methodological approach in this study, the aims and objectives must stay in focus. The aim outlined in Chapter 1, “to investigate the feasibility of measuring UES through remote sensing, using a methodology that is replicable across multiple cities, standardised so results can be compared between sites, and is efficient enough to be accessible to cities with limited resources” required a methodology that reduced potential variability of results between cities while keeping the protocols from becoming prohibitively complex. Thus, primary foci in the methodological development include simplicity of ES map development, streamlining of methods to reduce potential for bias or analyst error, consistent and uniform data sources, and minimal barriers to entry for researchers or urban planners interested in replicating this method. The methodology that follows is the synthesis of these factors into a replicable strategy for developing UES maps and assessing their accuracy.

### 3.2. Data Sourcing and Strategy Development

Because this research was aimed at cities across multiple states in the U.S., nationwide datasets were used for data consistency. To determine the research extent for each city, the United States Center for Disease Control’s “500 Cities: Cities Boundaries” shapefile was used (U.S. General Services Administration, 2020), which includes shapefiles for the boundaries of 500 of the largest US cities. For high resolution urban spectral data, the United States Geological Survey’s “National Map Data Download” application was used (USGS, 2022). This includes the National Agriculture Imagery Program’s (NAIP) 1m resolution aerial 4-band imagery dataset. Data was selected using the shapefiles from the “500 Cities: City Boundaries” dataset to define the extent of the data search. A complete footprint of the city extent, using the most recently published NAIP imagery, was downloaded in bulk using the UGet application provided by the National Map Data Download service.

In order to achieve the research aim of consistency in the methodology, user bias must be reduced as much as possible. Therefore, deep learning algorithms were investigated to create a consistent classification method across all cities. Among available AI-driven multiclass high-resolution landcover models, the “High Resolution Land Cover Classification – USA” deep learning model, developed as a collaboration between the USDA and Esri, accessed through Living Atlas (Esri, 2023a), was utilized. This classification model was selected for several reasons. First, the model was created and tested by ESRI, which is well-respected within the GIS community. Esri has also made it freely available on the Living Atlas database, which increases the accessibility of the model. It requires no supervised classification on the part of a geospatial analyst, thereby removing a potential source of variability. And despite the relative newness of the model, it has already been used in other peer-reviewed research (Haske, Tanya Brodie Rudolph and Bernsdorf, 2021). The classification categories were also compatible with some of the MAES Urban Ecosystem Services Providing Units (See figure 5). This model is designed for high resolution data (up to 80cm pixels), which is necessary for the spatial heterogeneity of the urban environment. Finally, the algorithm claims to be able to differentiate groundcover, shrub, and tree canopy layers of vegetation without the use of LiDAR data, which

MAES Urban ES Providing Units (JRC)	Deep Learning Landcover Classes (ESRI & USDA)
Forest, trees, shrubs	Water
	Wetlands
Vegetation, soil	Tree Canopy
	Shrubland
Forest, trees, shrub, herbs, lawns, wetlands, water bodies	Low Vegetation
	Barren
Forest, trees, shrubs, vegetated surfaces	Structures
	Impervious Surfaces
Trees, shrubs, vegetated and permeable surfaces	Impervious
	Roads
Wetlands	

Figure 5: Side-by-side comparison of the UES providing units outlined in the MAES 4<sup>th</sup> Report (Maes et al., 2016), and the landcover classes in the Esri/USDA Deep Learning Model (Esri, 2023a).

reduces the processing power necessary to generate appropriate landcover maps and further increases the accessibility of the methodology by removing the potential barrier of LiDAR data availability. Table 1 summarises data sources for this study.

Data Name	Use in Study	Type of Data	Source	Year released/ updated
500 Cities: Cities Boundaries	Defining City Extents	Shapefile	U.S. CDC	2020
NAIP Plus (1m)	Raw multispectral data for analysis	4 band aerial imagery (raster)	National Map Data Download, USGS	2016-2021 (depending on city)
High Resolution Land Cover Classification – USA	Landcover Classification Method	Python-based Deep Learning Package	Living Atlas, Esri Analytics	2022
MAES Service Providing Units	Categorization Protocol for Landcover Types	Urban Ecosystems Report	European Commission	2016

*Table 1: Summary table for data discussed in section 3.2.*

### 3.3. “Traffic Light” Ecosystem Service Matrix

As previously mentioned, a major shortcoming of the traditional ES matrix is that it requires contextualization at each city (Campagne et al., 2020). This prevents objective comparisons between cities due to the contextualization, while simultaneously creating another barrier of entry for cities interested in urban ES assessments, as contextualization has associated requirements of cost, expertise, and time. An ES matrix based on the MAES 4<sup>th</sup> report ES Providing Units that does not require individual site contextualization was created for this study.

The Service Providing Units as designated by the MAES 4th report were compared to the landcover classes in the deep learning model, and it was determined that six regulating ecosystem services could be estimated using the deep learning classification model. This number was reduced to five given the significant overlap between the categories of “Hydrological cycle and water flow maintenance” and “Flood control”. These five urban ES were combined with the landcover categories of the deep learning model to create the framework for the ES Matrix.

In order to address the challenge of contextualization, the spectrum of values assigned in the matrix were reduced to categorical assignments. A “traffic light” approach to the values assigned to given landcovers was developed, which assigned a value of “1” to a landcover that “directly provides the ecosystem service”, “0.5” to a landcover that “indirectly or partially provides the ecosystem service”, and “0” to landcovers that “do not provide the ecosystem service”. This approach, as opposed to the traditional 0-5 qualitative “value” of a given landcover in most ES matrices, means that the values can be transferred between cities, without developing specific qualitative values of each landcover type for each city. Figure 6 shows the first iteration of this style of ES matrix for initial experimentation.

**"Traffic Light" Assessment of Urban ES (MAES 4th Ed, CICES for Urban Environments)**

	Trees	Shrubs	Ground Vegetation	Soil/Barren /Pervious	Water	Wetlands	Built
Air Quality	1	1	0	0	0	0	0
CO2 Reduction	1	1	0.5	0	0	1	0
Urban Temp	1	0.5	0.5	0	1	1	0
Noise Mitigation	0.5	0.5	0.5	0	0	0.5	0
Water Flow	1	1	0.5	0.5	1	1	0

Figure 6: First iteration of the “Traffic Light” ES Matrix. 1 = Directly Provides ES, .5 = Indirectly/Partially Provides ES, 0 = Does Not Provide ES

When it came to determining whether a given landcover directly or indirectly/partially provided a given ES, a literature reviews was performed. For noise control, although all vegetation was considered noise reducing in the MAES Service Providing Units (figure 3), vegetation only can directly reduce noise when situated in appropriate locations in relation to the noise (Van Renterghem, 2019), so all vegetation types were counted as an indirect ES, because they only directly mitigate noise when appropriately placed. Ground vegetation and shrubs were counted as partially providing UHI mitigation because although they do reduce UHI through utilizing solar radiation and evapotranspiration, they do not offer the cooling effect of shading like trees do (Rakoto et al., 2021). CO<sup>2</sup> reduction is more robust in woody vegetation versus herbaceous groundcover (Davies et al., 2011), which is why low vegetation only partially provides CO<sup>2</sup> regulation. Finally, water management by low vegetation and pervious soil does not provide the same degree of rainfall management compared to larger plants (Säumel, Weber and Kowarik, 2016), so they were assigned only a partial value.

### 3.4. Geospatial Methods

All GIS data processing used ArcGIS Pro 3.1.2, and any geoprocessing tools or software features mentioned in this section are in reference to this software. The Deep Learning Libraries Installer for ArcGIS Pro was downloaded from Github (ArcGIS API for Python, 2023) and installed to expand the functionality of ArcGIS Pro to include Python-based deep learning models. All data was downloaded and analysed in the WGS 1984 coordinate system. For all GIS data and maps included in this report, the following sources are acknowledged: ESRI, USDA, and USGS for basemaps, ESRI and USDA for the deep learning model, U.S. CDC for city boundaries, and the U.S. National Agriculture Imagery Program for 1m multispectral images. Any data analysis occurring outside of a GIS environment was performed in Microsoft Excel 365.

To process the NAIP imagery as a cohesive dataset within the extent of a city, the NAIP files were first tiled using the “Mosaic to New Raster” tool. The tiled aerial imagery was then limited to the extent of the city limits using the “Extract by Mask” tool, limiting the extent by the “City Boundaries” shapefile. The resulting data layer, containing the 4-band 1m resolution NAIP imagery clipped to the extent of the city limits, was used as the raster input for the “Classify Pixels Using Deep Learning” tool. The downloaded deep learning package, “High Resolution Land Cover Classification – USA” was the defined model for the classification process.

Once the classification process was complete, the “Reclass” tool was used to change the landcover classifications to the associated values in the ES matrix. This was done five times, once for each of the UES being investigated in this study. With this tool, one can only assign integers as values, so instead of assigning values of “1”, “0.5”, and “0” (as in the “Traffic Light” ES matrix), the values needed to be changed to “10”, “5”, and “0”. Although these individual UES maps have value, they were then combined using the “Raster Calculator” tool. Using the “Raster Calculator” to sum the combined values from the individual UES maps, a combined UES map is formed, with values of 0 (built environment) to 45 (tree canopy).

The “Generate Random Points” tool was used, and random points were generated within the city’s extent. These points were given specific X, Y coordinates using the “Calculate Geometry Attributes” tool. The random points and the associated X, Y coordinates were then exported to

an Excel spreadsheet. These points were used as ground truthing points, to assess the accuracy of the deep learning model and generate F1 scores for the classification types.

This workflow was repeated for a total of 10 cities. Cities were selected based on their distribution across the Western United States and the presence of the city boundary in the “500 Cities: City Boundaries” shapefile. Figure 7 shows the Model Builder diagram for the workflow within ArcGIS Pro.



Figure 7: The Model Builder workflow in ArcGIS Pro for the Geospatial Methods in this study.

### 3.5. Data Analysis Methods

Fifty ground truthing points were assessed per city. Points were first identified based on the deep learning model landcover classification in which they appeared. Then, each point was digitally verified in triplicate, using the NAIP 1m imagery, Google Maps, and Google Earth Pro to verify what landcover type was actually present on site. Any time a point did not have a clear result across all three sources of aerial imagery, that point was skipped, and another point was assessed.

Mean accuracies per landcover category and per city were calculated. This was considered the “raw data”. After an initial data assessment, the ES matrix was adjusted based on the capacities of the model. Furthermore, landcover categories from the classification system that were functionally the same (e.g., “Impervious Surfaces” and “Structures”, which are both categorized as “Built” in the ES matrix) were combined. This was considered the “adjusted data” and referred to the accuracy of the model within the specific application of the “Traffic Light” ES matrix assessment. The mean accuracies per landcover and city were recalculated for the adjusted data. The geospatial methods from the “Reclassify” tool through the “Raster Calculator” tool were repeated to generate new individual and combined ES maps, to account for the adjusted data and updated ES matrix. Cities had their UES score calculated based on the mean per-pixel values of the combined ES maps to determine relative concentration of ES providing units.

Confusion matrices were developed for landcover classification accuracy of both the raw and adjusted data. Using the confusion matrices, the F1 score was calculated for each landcover type. This was done using the data in the confusion matrices and using the equation:

$$F1=2 * ((Precision * Recall)/(Precision + Recall))$$

F1 scores are considered the standard statistical method for assessing machine learning classification tools with multiple classifications, because they take into account the overall accuracy, the precision, and the recall of each classification type (Fujino, Hideki Isozaki and Suzuki, 2008). These values were then compared to the F1 scores initially published by Esri and USDA for each landcover classification in the deep learning model, to compare how the model in this application performed as compared to the original development.





## CHAPTER 4: Results

### 4.1. Raw Data

Figure 8 shows the accuracy per landcover type. The overall mean accuracy of all landcover types was 74.6%, with a standard deviation of 28.9. The coefficient of variation (CV) is 38.6%. Upon further investigation of the data, this wide CV and relatively low average is due to some notable outliers.

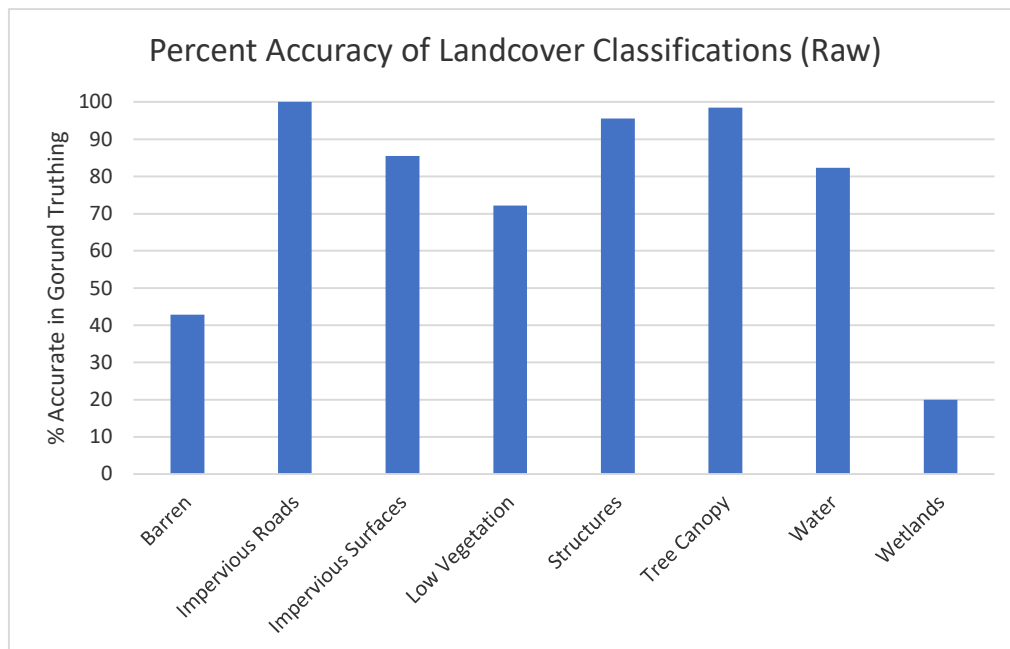


*Figure 8: Percent accuracy of each landcover classification in the raw data from the ground truthing accuracy assessment.*

All built environment categories had an accuracy above 85%. “Tree Canopy” had an accuracy of 98.5%, while “Water” had an accuracy of 82.4%. “Low Vegetation” had an accuracy of 72.2%, with 52.2% of the erroneous points categorized as “Low Vegetation” actually being shrubs or trees. Given these results, up to 14.6% of the “Low Vegetation” pixels in a given city may actually represent shrubs or trees, which have higher value as ES providing units.

The landcover classes with notably low accuracies include “Shrubland”, “Wetlands”, and “Barren” (exposed, unvegetated soil). In terms of the “Barren” class, the accuracy was 42.9%, and 67.7% of the erroneous pixels were actually impervious surfaces upon ground truthing.

The remaining 33.3% of errors were areas of sparse low vegetation. Although the groundcover did not completely cover the ground, these areas could not be truly categorized as “Barren”, because the overall landscape profile was impacted by vegetation. This was the case with much of the “Barren” classified pixels in Albuquerque and Los Angeles, which are both arid climates. Wetlands had a 20% accuracy, and only had 5 points included in the 500-point accuracy assessment. This class was also only present in three of the ten pilot cities. Because the deep learning model is proprietary and functions as a “black box”, one can only speculate on the mechanism used to categorize wetland pixels, but overall, this class appears to introduce significant error. All the erroneous pixels categorized as “Wetland” were actually “Low Vegetation”.

Finally, there were no “Shrubland” categorized pixels in the ground truthing points. “Shrubland” pixels only occurred in the classifications of six of the ten pilot cities, and only represented 1644515 of the 7918764507 pixels categorized, or .02% of the total area assessed in this study. It is interesting to note that 93% of the pixels categorized as shrubland occurred in Las Vegas, a particularly arid city.

Table 2 includes the F1 scores provided by Esri and USDA during the development of the deep learning model, as well as the F1 scores for the raw data. In general, the natural classes had a higher F1 score in the Esri/USDA data, whereas the built environment classes had a higher F1 score in this study. However, apart from the wetland class, there was less than a 15% difference between the Esri/USDA F1 scores and the F1 scores in this study. The range of F1 scores is from .33-.94, with a mean of .75, as compared to .8 for the Esri/USDA results. An F1 score of .8 and above is considered good for deep learning multiclass classifications, while above .9 is

### F1 Scores for Raw Data

Classification	ESRI/USDA F1	F1 from Raw Data
Barren	0.58	0.51
Impervious Roads	0.79	0.81
Impervious Surfaces	0.71	0.86
Low Vegetation	0.86	0.81
Structures	0.82	0.94
Tree Canopy	0.92	0.82
Water	0.93	0.9
Wetlands	0.79	0.33

*Table 2: F1 scores for raw data compared to the Esri/USDA F1 scores for the deep learning model.*

considered very good (Konstantinovskiy et al., 2021). “Barren” and “Wetland” are again the two main outliers in the F1 score analysis, with F1 scores of .51 and .33, respectively. This mirrors the results from the accuracy assessment, where these two classes had lower averages when assessing the ground truthing points. In the Esri/USDA F1 scores, the “Barren” and “Wetland” scores were .58 and .79, respectively. In both studies, the “Barren” class performed relatively poorly, whereas the “Wetland” class had an above-average score in the Esri/USDA data. If both of these classes are removed, the mean F1 score notably increases for both this study and the Esri/USDA data. For this study, the mean F1 score without these classes is .86 with a range of .81-.94 and a standard deviation of .05. For the Esri/USDA data, the F1 score without these classes is .84 with a range of .71-.93 and a standard deviation of .08. From this analysis, it can be stated that the F1 scores and therefore statistical accuracy of this study roughly align with the initial Esri results from the development of the model, with the exception of the “Wetland” class.

Figure 9 compares the accuracy of raw data on a per-city basis. The overall mean of per-city assessments is 83.2%, with a standard deviation of 2.5 and a CV of 3%. The range of accuracies was from 80-86%, and the mode is split between 82% and 86%. It should be noted that “accuracy” simply refers to the percent correct in the pixel classification, whereas the F1 score is a statistical assessment of the precision of the model.

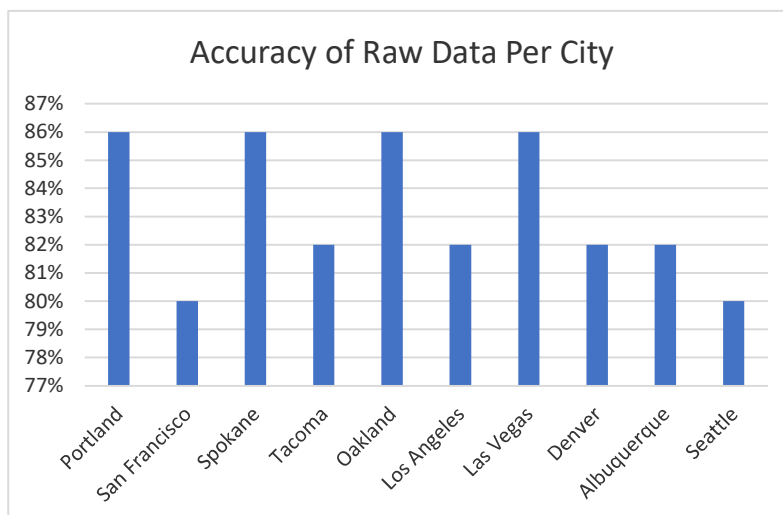


*Figure 9: Per-city pixel accuracy of raw data from ground truthing assessment.*

## 4.2. Adjustments to Methodology Based on Raw Data

Figure 10 highlights the changes made to the ES matrix based on the assessment of raw data. Given that 80% of pixels classed as “Wetland” were actually “Low Vegetation”, the values for “Wetland” pixels were adjusted to match that of “Low Vegetation”. Additionally, because of the low accuracy of the “Barren” class and the high incidence of the deep learning model categorizing “Impervious Surfaces” as “Barren”, “Barren” pixels were assigned a value of “0” to reflect the likelihood of these areas being built environment. For the accuracy assessment of the adjusted data, “Wetland and “Low Vegetation” are a combined category, and barren and impervious surfaces are also a combined category. Finally, because the “Shrubland” class was so poorly represented across all maps, and was not represented at all during the ground truthing, the adjusted data includes a class called “Tree/Shrubs”, to better represent the likelihood of these two classes overlapping. The rare cases of “Shrubland” classes in the maps was left to increase the potential data resolution of the ES maps. In chapter 5, the implications of these changes to the ES Matrix will be discussed.

Original							
	Trees	Shrubs	Ground Vegetation	Soil/Barren /Pervious	Water	Wetlands	Built
Air Quality	1	1	0	0	0	0	0
CO2 Reduction	1	1	0.5	0	0	1	0
Urban Temp	1	0.5	0.5	0	1	1	0
Noise Mitigation	0.5	0.5	0.5	0	0	0.5	0
Water Flow	1	1	0.5	0.5	1	1	0

Edited Based on Ground Truthing							
	Trees	Shrubs	Ground Vegetation	Soil/Barren /Pervious	Water	Wetlands	Built
Air Quality	1	1	0	0	0	0	0
CO2 Reduction	1	1	0.5	0	0	0.5	0
Urban Temp	1	0.5	0.5	0	1	0.5	0
Noise Mitigation	0.5	0.5	0.5	0	0	0.5	0
Water Flow	1	1	0.5	0	1	0.5	0

Figure 10: Original and edited “Traffic Light” ecosystem services matrix, updated to reflect the potential limits of the deep learning model.

It is also important to note that some of the errors in the ground truthing process were classes of built environment being categorized as a different kind of built environment. When it comes to the development of an urban ES map, these errors do not impact the accuracy of the final assessments. Therefore, in the adjusted data accuracy assessment, all built environment categories (“Impervious Surfaces”, “Impervious Roads”, and “Structures”) were counted as a single class of “Built”, which will also include any “Barren” pixels.

### 4.3. Adjusted Data

Figure 11 shows the average accuracy per adjusted landcover class. The adjusted data had a mean accuracy of 87.6%, with a standard deviation of 10.5 and a CV of 11.9%. This is a notable improvement in accuracy and statistical performance as compared to the raw data. The only class with less than 80% accuracy is “Low Vegetation”, which only increased to 73% with the combination of the “Low Vegetation” and “Wetland” classes. The “Impervious/Barren Soil” category reached an accuracy of 96.5%. Accuracy of “Water” and “Trees/Shrubs” remained unchanged.

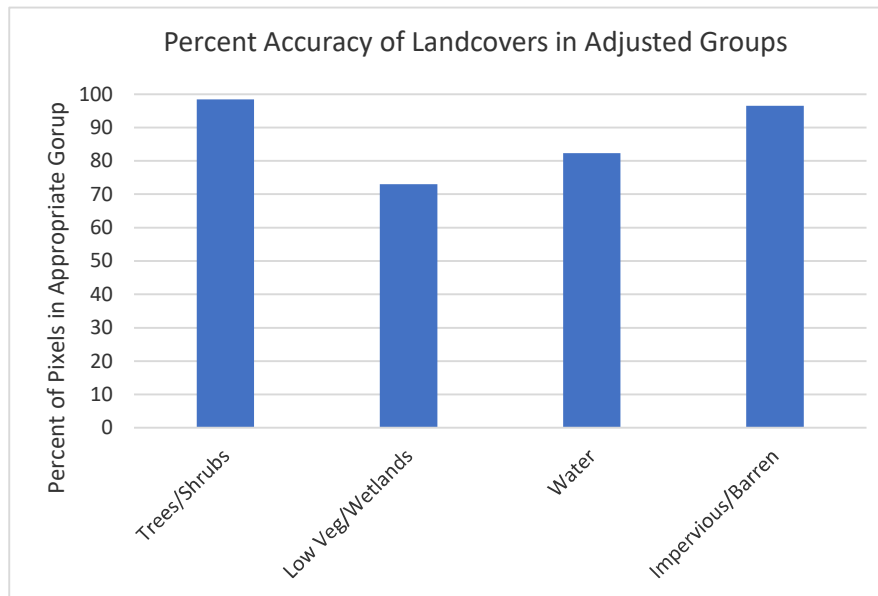
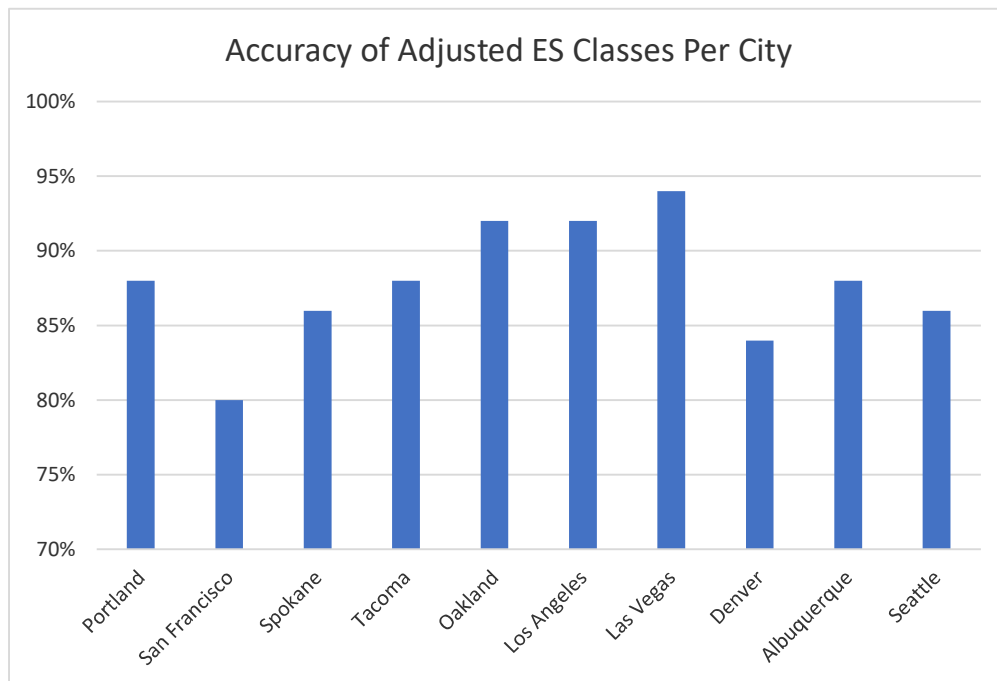


Figure 11: Percent accuracy of landcover pixels of adjusted data after grouping pixel types.

Because the “Forest/Shrubs” and “Water” classes had no changes in pixel categorization from the ground truthing process as compared to the raw data, their F1 scores are the same as in the

raw data. For the “Low Vegetation/Wetlands” and “Built Environment/Barren” classes, there was an improvement in F1 scores (.82 and .94, respectively). The new mean F1 score for the adjusted data is .87, with a range of .82-.94 with a standard deviation of .06. Therefore, when the classification management is adjusted to reflect the results from the initial assessment of the raw data, the deep learning model can be considered a statistically accurate landcover classification tool for this application.

As can be seen in figure 12, the mean per-city accuracy of the adjusted data reached 88.8%, with a standard deviation of 3.1 and a CV of 3.6%. The range of accuracies was from 84-94%. Given this high accuracy and low coefficient of variation, this can be an effective tool for assessing the distribution of five UES across a variety of urban environments.



*Figure 12: Per-city pixel accuracy of adjusted data.*

#### **4.4. Urban Ecosystem Service Values for Pilot Cities**

Beyond the accuracy assessment of the deep learning model in relation to the novel standardised ES matrix, it can be helpful to understand the distribution of values generated by the model. Figure 13 shows the combined ES map and average score for a single city (Portland, OR), while figure 14 includes the successive map generation process for determining the overall ES value for Portland. Appendix A shows the combined ES maps for the 10 pilot cities



along with the mean per-pixel value for the city extent. The range of values was from 7.68 in Albuquerque, NM to 17.79 in Portland, OR. The mean for the ten cities is 12.08, with a standard deviation of 3.31. When separated into broad environmental categories (Portland, San Francisco, Tacoma, Oakland, and Seattle as temperate; Spokane, Los Angeles, Las Vegas, Denver, and Albuquerque as arid), there are some differences. The temperate city average is 13.64 with a standard deviation of 3.31, and the arid city average was 10.53 with a standard deviation of 3.87. Because this is a dimensionless metric, it cannot necessarily be used to quantify specific benefits. However, it can be very useful for comparisons between cities or understanding relative distributions within a city. In chapter 5, methods for increasing the usability of these numbers by urban planners and policymakers will be discussed.

All tables for the ground truthing process and, as well as confusion matrices and data analyses can be found in Appendix B.

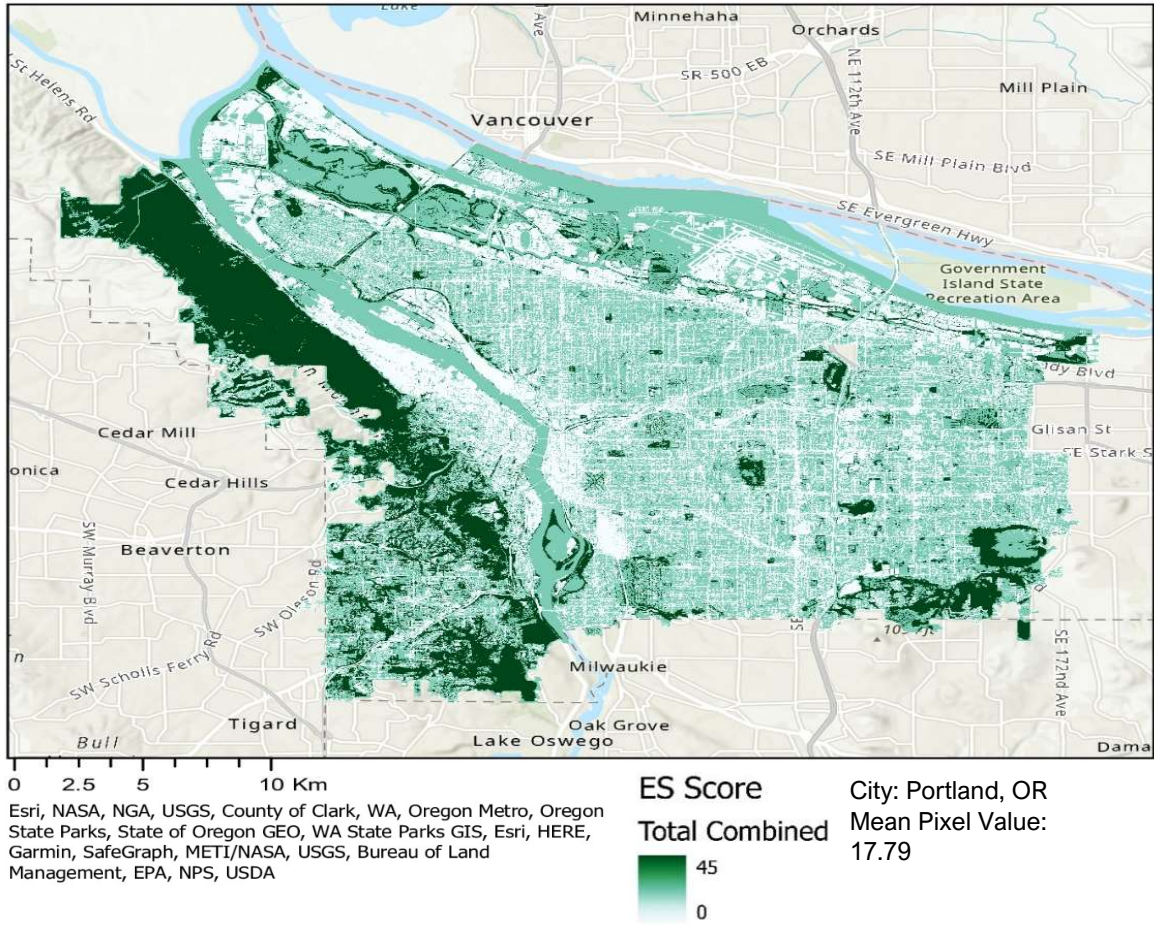


Figure 13: Combined ES map for Portland, OR. This was the city with the highest average overall ES value, with a score of 17.79.



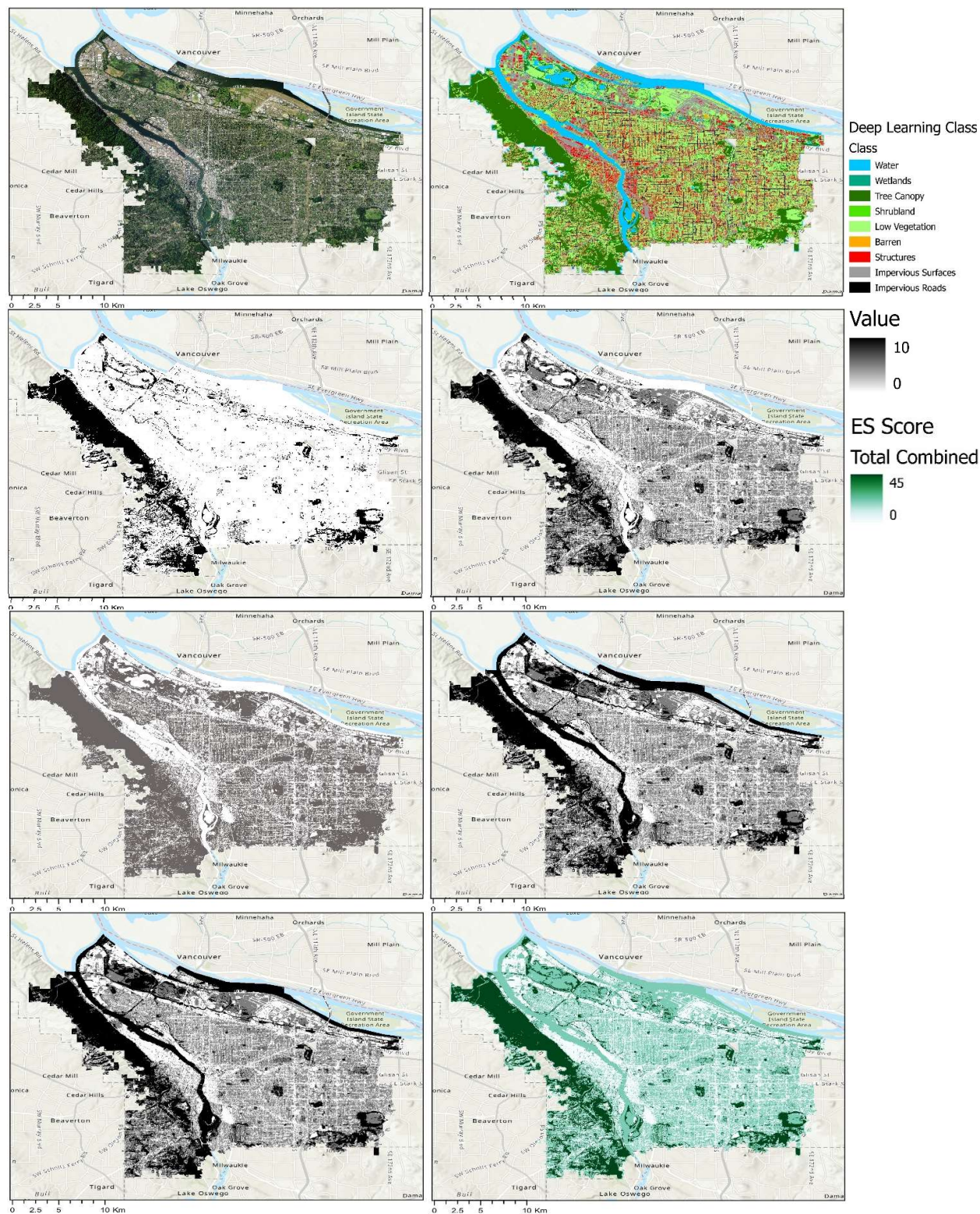


Figure: Results of successive map generation to create a final combined ES map. 1) NAIP Aerial Imagery, 2) Deep Learning Classification 3) Air Quality ES Layer, 4) CO2 regulation ES layer, 5) Noise Mitigation ES Layer, 6) Temperature Regulation ES layer, 7) Water Management Layer, 8) Total Combined ES Map



## CHAPTER 5: Discussion

### 5.1. Results Summary and Significance

Grekousis found a mean of accuracy 87.1% in AI landcover classifications (2018), and this study produced similar results. Given the high accuracy (84-94%, average of 88.8%) and low CV (3.6) of the per city analysis of adjusted data, this particular deep learning model could be an effective starting place for the development of a standardised methodology for nationwide urban ES assessments in the United States, with the potential to be applied internationally as well. The adjusted data's F1 score range of .82-.94 and mean of .87 supports this claim. This study only looked at five of the regulating ecosystem services outlined in the MAES 4th report, and a complete ES analysis would require additional data beyond aerial imagery, but this methodology is simple enough to be accessible to many city governments with access to geospatial analysis tools, and the data required is readily available for most urban areas across the United States.

This novel approach to an ES matrix also removes the need for location-specific contextualization. The units in most ES matrices are already dimensionless units, so they are descriptive and comparative rather than directly quantitative to begin with. Furthermore, the individually contextualized ES matrices limit the applications to research or policy within the city's extent, and therefore cannot contribute to regional or federal policy or research. Finally, as mentioned in the literature review, many ES matrices copy their values from Burkhard et al.'s ES matrices which are contextualized to Northern Germany (Campagne et al., 2020), and so the contextualization can be a hinderance to policy development in other climates.

Although in this research the ES matrix units are also dimensionless, the categorical value system means that values of a given area can be more easily understood. The values are directly tied to literature reviews and the standards developed in the MAES 4th report. The methodology is also fluid enough that if a particular municipality has the desire or resources for an ES assessment that is contextualized to the city, the same data and methods can accommodate city-specific valuations of ES. The municipality would only need to change the values in their own ES matrix and rerun the "Reclass" steps in the methodology. This allows a

city to give greater priority to a given landcover classification or ES type if it suits their purpose.

This methodology also has the benefit of having a very low entry barriers for individual cities to replicate. Depending on the size of the city, it took 2-5 days of processing on a single computer (processor: Intel(R) Core(TM) i7-9700 CPU at 3.00GHz, 64GB Ram), with one supervising geospatial analyst to complete the methodology. The data was all free, and the deep learning model is accessible to anyone with an Esri Living Atlas membership. Additionally, because the pixel classification is performed by deep learning, it has a consistent approach to the classification process across multiple cities. Whereas with a supervised classification approach managed by geospatial analysts, there would be inevitable variability in the classification training process based on differences in training area selection by each analyst. Replacing the often-iterative process of pixel training for the deep learning model decreases variability, time, technical experience with supervised classifications, and analyst bias from the process of remote-sensing based UES assessments.

## **5.2. Limitations**

When developing new methodologies, understanding the limitations can be as important as understanding its application. Despite the successes of this model outlined above, its shortcomings must be discussed. They are primarily limitations with the model, but they also include limitations of remote sensing for certain landcovers and ES, as well as data limitations.

### **5.2.1. Barren Soil**

As mentioned in Chapter 4, the accuracy in detecting barren soil in the ground truthing process was 42.9%. Barren soil was identified as a potential provider of water management in cities, as the permeable surface allowed for stormwater to infiltrate. However, the model was not successful in identifying barren soil in this study. The F1 score of .51 for the “Barren” class highlights this shortcoming, indicating that this class was not well identified in the multiclass assessment. These results were echoed in the F1 scores released by Esri/USDA in their technical review of the model, where “Barren” had an F1 score of .58 (Esri, 2023a). In the ES matrix for this study, barren soil was only identified to provide partial water management (a

value of .5). Furthermore, barren soil was primarily only identified accurately in arid climates (Albuquerque and Las Vegas), with the exception of 1 correctly identified pixel in a temperate city (Tacoma). Therefore, this inaccuracy in the model only has minor implications, since water management is often less of a concern in arid climates. Nevertheless, ignoring the benefits of permeable soil and assigning them a value equal to that of a paved surface could lead to poorly informed land management. This will also further skew for lower ES values and increased error in arid cities, as they tend to have more unvegetated exposed soil.

### **5.2.2. Wetlands**

The other major change to the ES matrix after assessing the raw data was the “Wetlands” class. With an accuracy of 20%, and all erroneously identified pixels actually falling in the “Low Vegetation” category, it was more accurate to the ground truthing results to match “Wetland” pixels to the values of “Low Vegetation”. This class also had the lowest F1 score of .33, which was less than 65% of the next lowest F1 score. The wetland category in the ES matrix had impacts across four of the five regulating UES in this study, and its values were different than ground vegetation in three of those four UES. So, combining the “Wetland” and “Low Vegetation” pixels to a unified value in ES mapping could lead to serious under-representation of regulating UES, especially in coastal or riparian cities where wetlands are common.

Wetlands can be a challenging category for remote sensing classification, because although they have their own unique ecosystem function, they can have a variety of vegetation structures and aerial photography struggles to discern differences in soil conditions. Furthermore, ephemeral water bodies that are common in wetlands can be challenging to identify when there are not multiple time-points in the geospatial analysis. However, U.S. federal policy requires urban wetland delineation to reduce the potential impact of development on wetlands (Tiner, 1993). As a result, many cities already have wetland delineation maps. If these wetland delineation maps are already stored as shapefiles, then the wetland shapefiles could be included in the geospatial assessment, and any pixels that intersected the wetland shapefiles could be reclassified as “Wetland” pixels, dramatically improving the accuracy of the ES assessment. Any “Wetland” pixels not intersecting the city’s wetland shapefiles could be reclassified as “Low Vegetation” (or another class based on the geospatial analyst performing ground truthing), and the wetland values from the original ES matrix could be used, thus creating a more complete and accurate assessment of UES.

### 5.2.3. Albuquerque – Impacts of Adjusted Data

The city of Albuquerque, NM was chosen as a case study to investigate the potential error introduced from the edits made to the ES matrix following the analysis of the raw data. Albuquerque was chosen because during the ground truthing, it had the most “Barren” class pixels, and it had the one correctly identified “Wetland” pixel.

Figure 15 compares the landcover classification map of Albuquerque with the “raw data” overall ES map and the overall ES map after adjusting the ES matrix. Prior to adjustment, the overall city pixel average for the city is 8.60. After the matrix adjustment, the city pixel average dropped to 7.68. The city extent totalled 686049889 pixels, and included 3675246 “Wetland” pixels and 116151145 “Barren” pixels. This equates to .5% of the total map classified as “Wetland” and 16.9% of the map classified as “Barren”. After receiving new ES matrix values, this introduced a roughly 11% decrease in average pixel value for the city. Of particular note is the “Wetland” and “Barren” pixels near the Rio Grande (circled in black in figure 15). Given the increased impact on the water management UES from the changes in pixel values, and the increased need for water management ES near the Rio Grande, this is an example of where the changes in pixel value could lead to improper policy development. The importance of the wetlands near the Rio is reduced, and barren soil is valued at the same level as a parking lot. This means that a policymaker using this map could inadvertently under-prioritize these areas during climate-conscious planning.

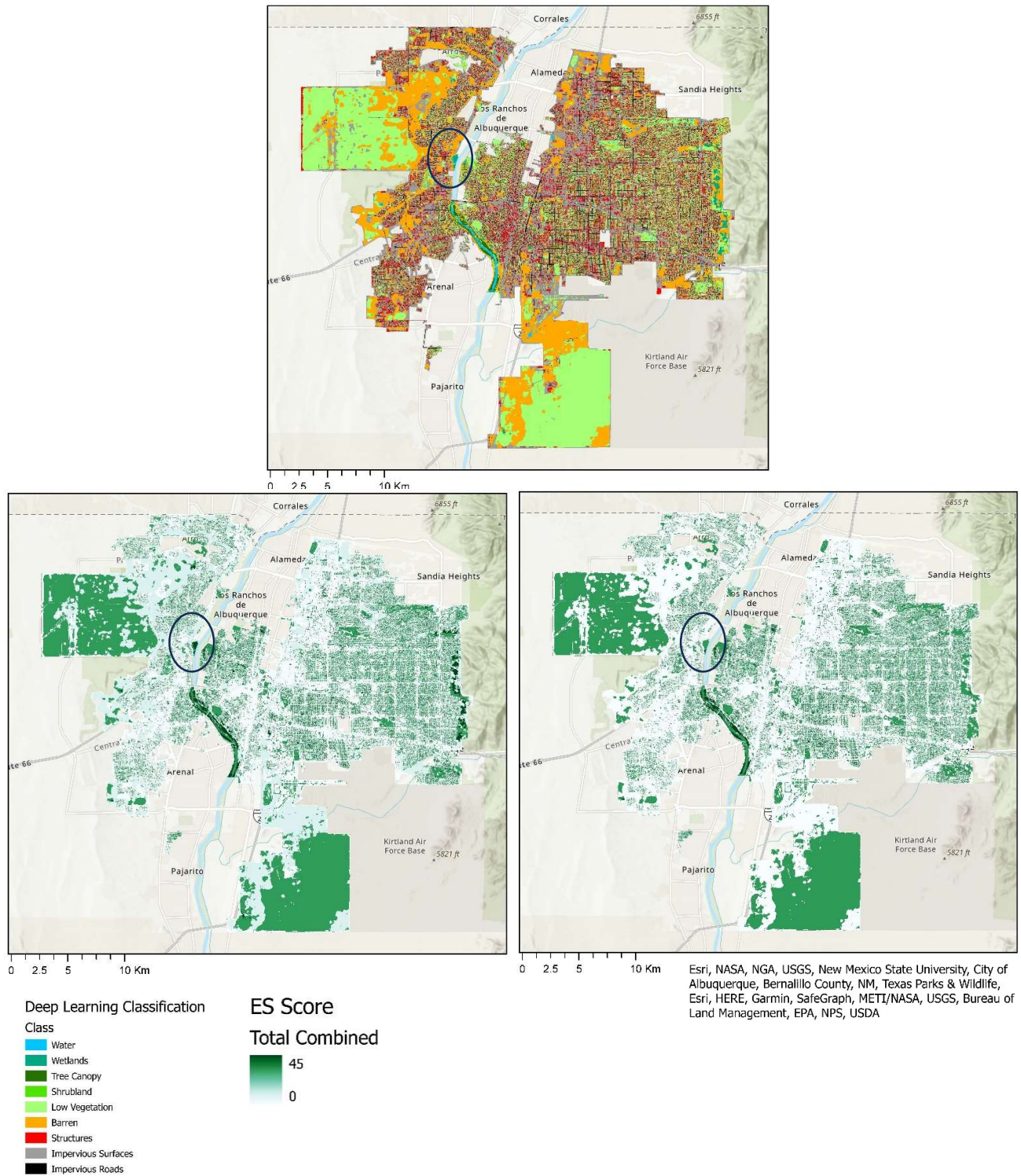


Figure 15: Albuquerque model classification map (top), and combined Ecosystem Service values for raw data ES Matrix (lower left) and adjusted ES matrix (lower right). Black circle indicates the area of “Barren” and “Wetland” pixels near the Rio Grande where water management ES is critical but the deep learning limitations lead to a reduced presence of water management ES in the area.

#### 5.2.4. “Tree Canopy” vs “Shrubland”

Because the deep learning model had separate classes for “Tree Canopy” and “Shrubland”, it was assumed that the model could separate shrubs from trees using just aerial imagery. However, given the low presence of shrubland pixels across all pilot cities (.02% of all pixels in the study), and that none of the ground truthing points landed on a “Shrubland” pixel, the accuracy of the “Shrubland” class cannot be assessed. As such, it must be assumed that the category cannot be confidently separated from the “Tree Canopy”. Furthermore, at the time of this writing, the model developers do not have a publicly available document with a classification description that specifies the exact differences used to define “Tree Canopy” versus “Shrubland”. In the Esri/USDA publication of the model, the “Shrubland” class only had an F-1 score of .27, the lowest of all categories. This further supports the removal of this class for ES assessments.

When it comes to the ES matrix, there is only one ES where the values for trees and shrubs are different: UHI. It could be argued that depending on the size of the shrub, taller shrubs may also provide shading and further decrease UHI (in the multimodal manner that trees do, as discussed in Chapter 3), but given the ambiguity of the classification, that assumption cannot be made. Because there were no “Shrubland” pixels in the ground truthing process, any vegetation with a notable vertical component was considered “Tree Canopy”. Therefore, shrubs which do not provide the same amount of shading as a “Tree Canopy”, received the value of “Tree Canopy” in the ES matrix “Reclass” step. Therefore, there is additional potential for error in the UHI ES, as UHI mitigation might be overestimated because of shrubs classified as “Tree Canopy”.

One potential solution for differentiating trees from shrubs is the inclusion of high-resolution LiDAR in the geospatial assessment. Applying LiDAR to the vegetated areas of the landcover classification would allow the analyst to measure heights of vegetated areas, further differentiating trees, shrubs, and groundcover. Unfortunately, LiDAR data processing requires high levels of data storage and extremely high processing power to do any assessments at a community level, let alone a full city. During this study, another deep learning model aimed at mapping individual trees (Esri, 2020) was applied to just the vegetated areas of the Los Angeles map. This analysis could not be completed, because the estimated time for the deep learning model to run with the computer specifications outlined above was over 75 days. When a smaller



case study neighbourhood of only a few blocks was investigated, it took three days to complete. The model only differentiated lidar pixels above 20 feet (6.1 meters), which would miss shorter trees and could not differentiate shrubs from groundcover. Given that the aim of this research was to develop an accessible and replicable ES assessment, multiple deep learning models and the introduction of LiDAR data would significantly increase the entry requirements for using this method. Therefore, that research was not included in this paper. However, that is an option for cities where shading is critical and urban planners need heights of vegetation for planning purposes.

### 5.2.5. Shadows – Seattle Skyscrapers

One major error can be seen in figure 16. When zoomed in to just the area of the ground truthing pixel, the area appears to look like water, which is how this area was categorized by the model. However, upon zooming out, it is clear that this is a large shadow cast on black asphalt by a skyscraper on a sunny day. In fact, the majority of the pixels that were shadows from the cluster of skyscrapers in the urban core of Seattle are not identified correctly. It makes sense why this error occurred, because the spectral signature of shadows on black asphalt is very similar to water.

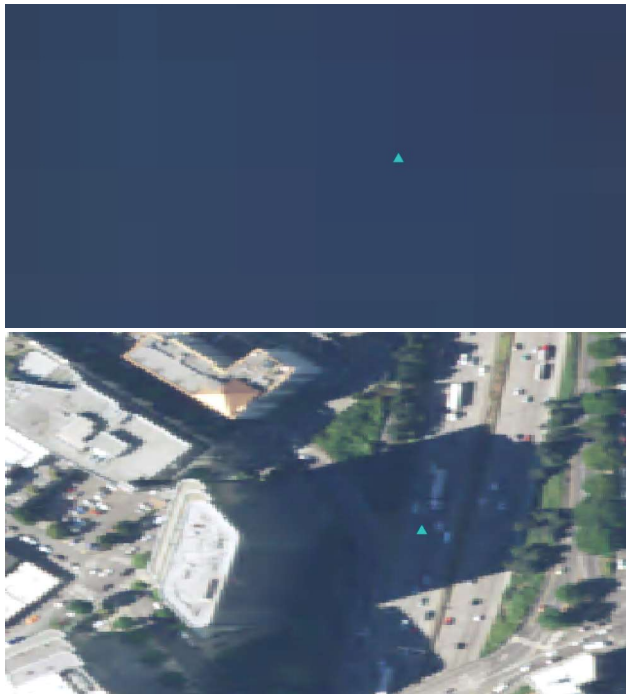


*Figure 16: Seattle skyscraper shadows that were categorized as water. Top photo is zoomed in on the area categorized as water, bottom photo is the shadowed area with the surroundings for context. The blue triangle represents the pixel selected for ground truthing.*

It is possible that an object-based classification could have avoided this better than the pixel-based classification that the model uses. Because object-based classification includes another layer of machine learning to complete, it can potentially increase accuracy and better define the specific delineation between different objects. However, it requires more processing power, and the current highest-resolution landcover classification model that was freely available was pixel-based. As models continue to be developed, it is possible that a future classification model for this application could be object-based.

This particular error also brings into consideration the role of the analyst. While in this approach, avoiding excess involvement by individual analysts was assumed to create results that are more consistent between cities, because analyst differences and biases are removed. However, the error associated with the Seattle skyscraper shadows is a large and obvious error that would be easily caught by an analyst familiar with the area. One potential solution would be for a local geospatial analyst to review landcover maps after the model has developed them, but before ES values are assigned. This way, the analyst does not have an opportunity to change the classification training within the model, but can still increase accuracy by catching major errors in the pixel classification.

#### **5.2.6. Temporal and Spatial Resolution Limitations**

This method relies on 1m resolution multispectral data, which is freely available for most of the United States. Unfortunately, this is not as widely available in other countries. The U.S. leads the world in publicly available GIS data (C. Daly et al., 2000), and therefore, data of this resolution might not be available in countries with lower GIS data availability. The data may also exist but be behind a paywall.

Data of this resolution also may not get updated as regularly as data with lower spatial resolution. Although older data can be used for initial assessments, ground truthing can be challenging when the current site conditions do not match the spectral data. It can be difficult for the analyst to tell if the model incorrectly classified a pixel, or if the specific location has been changed or developed since the spectral data was collected. Although this limitation was not as much of an issue with American data, and will become increasingly irrelevant as global GIS databases expand, it is important to acknowledge this potential error if this methodology is to be applied on a global scale.



### 5.2.7. Edge Effect and Error

Some of the erroneous ground truthing points were near the edge of the city extents. It is clear that the edge effect, a common source of error in environmental research, may also be impacting the accuracy of the model. Figure 17 shows a ground truthing point for the city of Tacoma, WA, near the edge of the city's extent. As can be seen from the aerial photography, the edge of the city extent is primarily forest, with a small building reaching the edge. However, the categorized the edge area as a mix of "Impervious Surface", "Structures", and "Water". These are highly unusual errors, as "Tree Canopy" was one of the highest accuracy landcovers. Figure 18 shows the edge of the urban extent of Portland, OR, which is clearly dominated by forest. In the landcover classification, it is clear that there is a band of inaccurate pixels, mostly "Water" classes, that introduces a notable amount of error into the model. There is a simple fix for this issue, which will be discussed in section 5.4.1, but this source of error had to be acknowledged given its impact on overall ES scores.

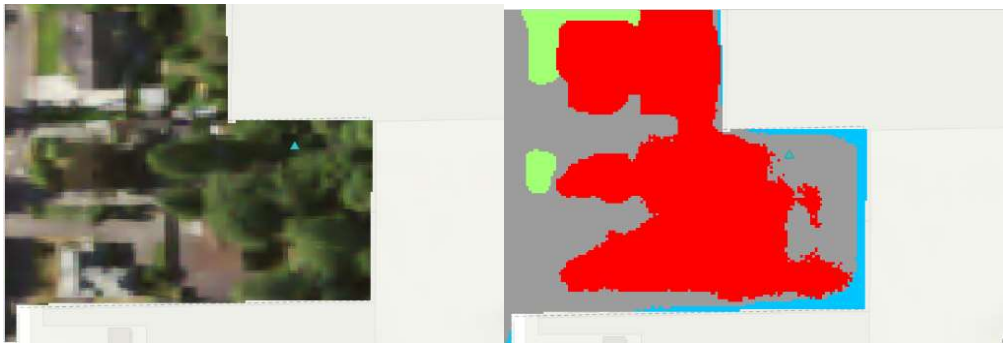


*Figure 17: Edge effect error in Tacoma, WA. The forests along the edges of the imagery are classified as "Structures" (red), "Impervious Surfaces" (grey), and "Water" (blue).*

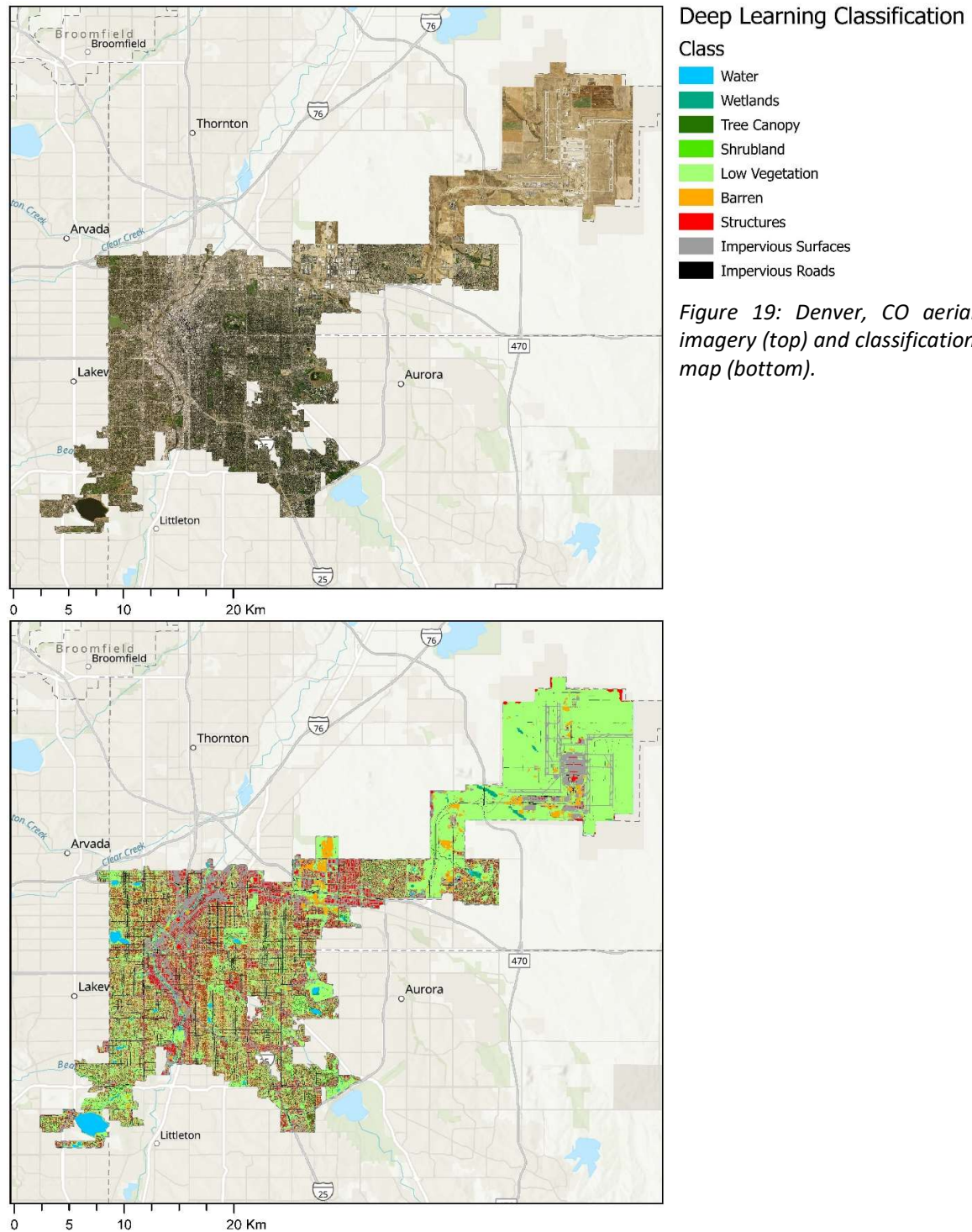


*Figure 18: Edge effect error in Portland, OR. Forests along the edge are classified as "Water" (blue) and "Structures" (red).*

### 5.2.8. Variability of Accuracy Between Cities

The range of overall accuracies between cities was 84-94%, with an mean of 88.8% and a CV of 3.6%. Although this is a low CV, the differences in accuracy between cities should be investigated, with particular attention to potential causes of the differences. The training site for the development of the deep learning model was the Chesapeake Bay Inlet along the East coast of Vermont, United States (Esri, 2023a). So although the model is advertised to process high-resolution data for all of the USA, the conditions where the model was developed are that of a coastal temperate environment. Because of this, it could be assumed that there is a greater potential for error in climates that are dissimilar to the training site. Unfortunately, because the model is a “black box”, in which the user of the tool doesn’t know the exact mechanisms applied, it is more challenging to troubleshoot the shortcomings of the tool beyond informed speculation.

The three cities with the lowest accuracies are Denver CO (84%), Spokane WA (86%), and Seattle WA (86%). For Denver, 70% of the errors in ground truthing were pixels that were inaccurately classified as “Low Vegetation” (See Appendix B). Of those pixels, 43% were “Tree Canopy” and 43% were “Impervious Surfaces”. Because Denver is an inland continental city, it is possible that the tree species are different enough from coastal temperate trees that the spectral signature of trees in Denver do not match the spectral signature of trees from the training site. Figure 19 shows the NAIP aerial imagery and classification map of Denver. The separate area in the Northeast of the city extent is the Denver Airport. As can be seen in the aerial imagery, the grassland identified areas in that area of the map are brown, and are represented by dead grassy areas around the airport in the summer. The dryness of these grassy areas may also have introduced error because the “Low Vegetation” in a coastal temperate area are more likely to stay green throughout the year. Similar potential explanations for Spokane could be considered, as Spokane is also an inland, dryer, continental climate. The distribution of errors for Spokane was similar to Denver, predominantly misclassified “Low Vegetation”, which was actually “Tree Canopy” and “Impervious Surfaces”. Seattle’s errors can potentially be attributed to the edge effect and the challenges with the skyscraper shadows, which are both discussed earlier.



It is interesting to note that Spokane and Denver, which have similar climates, were some of the most inaccurate sites. However, sites like Las Vegas and Los Angeles are arid and had high accuracies (94% and 92%), despite being more dissimilar to the Vermont model training site than Denver and Spokane. It is possible that these desert cities may have higher percents of

built surfaces, which had the highest average accuracy of any class. Indeed, Los Angeles and Las Vegas were the two cities with the highest number of ground truthing points in built classes (32 and 38 points in the adjusted classes, respectively). This could mean that these cities just have more built areas, and therefore were more accurately assessed by this model. Alternatively, repeating this research with a higher amount of ground truthing points per city could highlight other potential trends in accuracy between cities.

### **5.3. Applications**

To reiterate, the aim of this research is to investigate the feasibility of measuring UES through remote sensing using a methodology that is replicable across multiple cities, standardised to allow comparisons between cities, and is accessible to cities with limited resources. Although it only focuses on five of the seventeen UES identified in the MAES 4th report, it covers the majority of the regulating ES, which are of particular importance to the liveability of cities. The purpose of this methodology has two components. Firstly, urban planners and policymakers can better understand the distribution of ES within a city. This can be done with the combined ES maps, or the maps for individual ES that are generated in the “Reclass” step of the methods. The users of the data can then divide the city by a number of different factors to better understand which residents have a greater supply of ES in their neighborhood. Useful divisions can be based on neighbourhood, postal code, districts, or development zones. The average overall pixel value for a city or neighbourhood can also be divided by the population of the area for a per capita ES assessment. This would provide a rough understanding of the relationship between supply and demand of urban ES in a given area., which could act as a simplified proxy for a UVST assessment or ecosystem footprint estimations.

Issues relating to environmental justice can also be investigated with this tool. It is well documented that minority populations or poorer communities often have less access to urban green space and UES(Calderón-Argelich et al., 2021). As climate change brings more severe weather events such as flash floods and heat waves to cities, regulating ES will be increasingly seen as a lifeline for urban dwellers, as these ES buffer communities from economic or health-related impacts of extreme weather. Therefore, to ensure that historically disenfranchised communities do not continue to suffer disproportionately from the impacts of climate change, ensuring an equitable distribution of regulating ES throughout all communities will be

necessary. The spatial data generated in this method can be compared to demographic data, and data-driven policy can ensure that green space acquisition or development projects are directed at neighbourhoods that are both lacking regulating ES and include historically marginalized communities. This can benefit the city by protecting the most risk-prone communities from climate disasters, while ensuring that current green-development projects do not create deeper disparities between privileged and marginalized communities, creating a cycle of disenfranchisement and sociocultural segregation.

Beyond assessments within an individual city, this methodology further allows for comparative analyses of regulating ES between different cities. At the date of writing, the author found no studies that compared multiple types of ES across several American cities with a single unit of measure. In order to develop state or federal policy to protect, enhance, or expand urban ES, there needs to be a standardised unit for describing levels of ES present in multiple locations. And as the EU moves towards global mapping of ES (Burkhard and Maes, 2017), urban areas will inevitably be a bottleneck for the process. This methodology would allow for an initial mapping of some of the main ES that are relevant in the urban area to fill those data gaps. Regulating ES are some of the most relevant to the urban environment, because most provisioning ES come from outside the city. Therefore, it would be sensible for them to be a first step in mapping UES on an international scale.

An added benefit of this methodology is that it is flexible enough to incorporate other types of data for a deeper analysis of UES on a city scale. For example, if a city has mapped public green or open areas for the parks department, these shapefiles can be included in order to calculate the relative presence of nature-based recreation available in a city. With this same approach, heritage or culturally important sites can also be uploaded on a per-city basis for a more robust analysis of cultural ES. Viewshed analyses for vistas or heritage sites can also be calculated in ArcGIS, which can calculate areas that may partially provide cultural ES. Watershed analyses in ArcGIS can be used for methodologies to estimate provisioning ES related to water resources within the city if DEM data is available. And if the city maps allotments and urban or peri-urban farms, there is the possibility to incorporate those shapefiles for food provisioning ES. Finally, by including the wetland delineation shapefiles noted in section 5.2.2, this city-specific data can create a much more complete mapping protocol for UES. There is the potential for the “Traffic Light” ES matrix to be expanded to include all UES and Service Providing Units outlines in the MAES 4<sup>th</sup> report, and examples such as those above



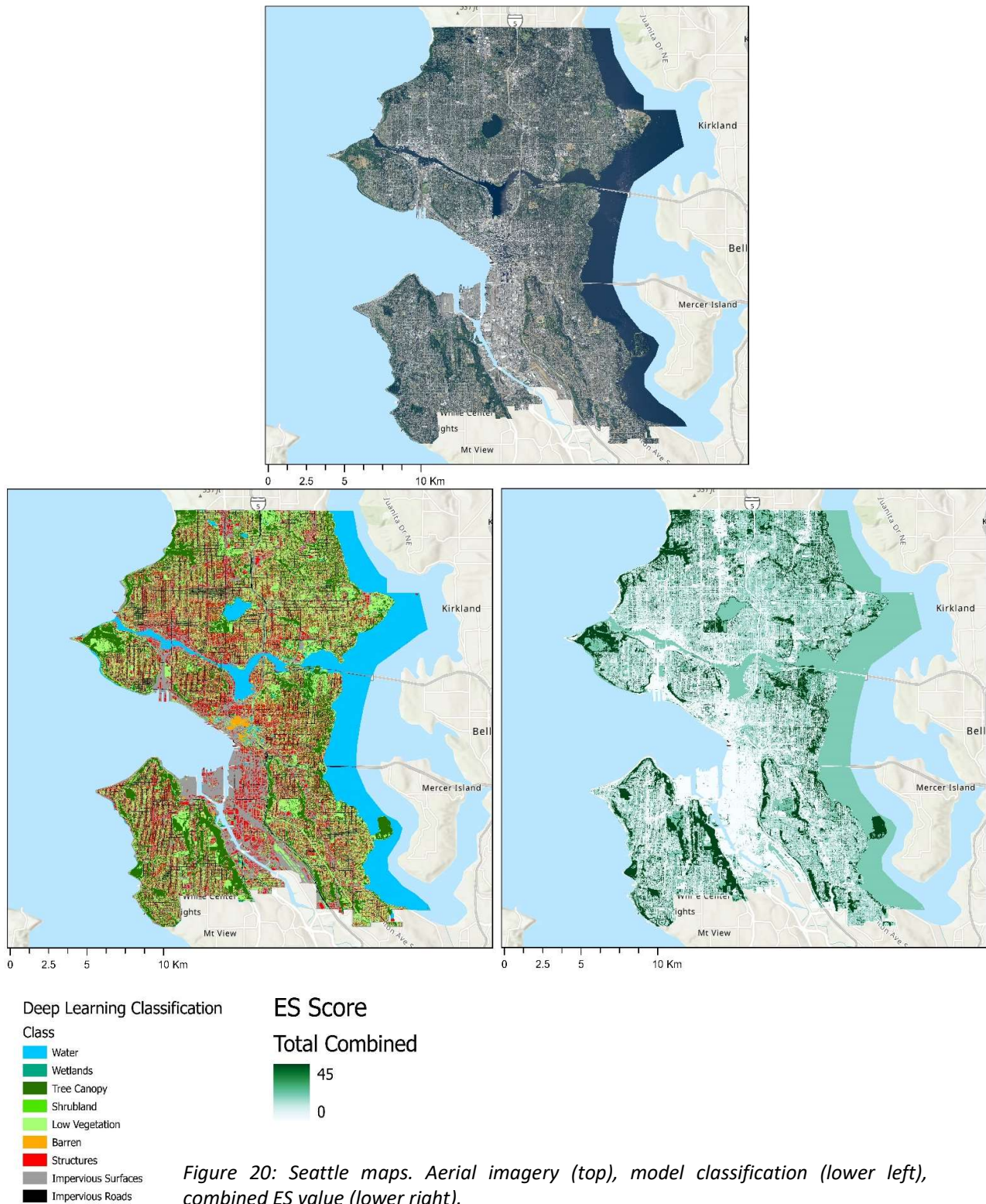
can be used to continue populating the the matrix with new values and data sources available at the municipal level. This could allow the methodology to evolve such that it can provide assessments for a full UES analysis, including combined UES values or smaller assessment for just cultural, provisioning, and regulating ES.

## **5.4. Future Research and Recommendations**

### **5.4.1. Specific Changes to Methodology**

There are several paths of investigation for future research directly related to this methodology that could result in improved outcomes in later iterations. One important factor is how edges of cities are defined in ES mapping. One example of this can be seen in Denver, CO. As discussed in 5.2.8 (see figure 19), the airport is included in the ES assessment. However, in terms of policymaking and spatial planning, the grasslands around the runways likely do not contribute much to the wellbeing of the residents of the city of Denver. One could postulate that the lack of trees around the airport (which the map did highlight) contributes to air pollution in the area, as “Low Vegetation” does not provide air quality ES. However, these negative impacts of the airport affect the smaller cities around the airport, as opposed to the residents of Denver. Therefore, it might be more useful for policymaking if the airport was included in the ES assessments of the smaller towns that are geographically related to the airport.

Additionally, as can be seen in figure 20 (Seattle, WA), coastal cities had their extent delineated to end before before the ocean began. This means that the positive impacts of the ocean did not get accounted for in the ES mapping. Freshwater resources were also not equally accounted for in the mapping process. Figure 20 shows how the Duwamish river, which goes through the South of Seattle but is still connected to the ocean, was not included in the city’s extent in the “500 Cities: City Boundaries” shapefile. However, Lake Washington, to the East of Seattle, was included to about halfway across the water body. It is not clear how water bodies are delineated in the shapefile, but developing a more consistent method of city delineation that provides an accurate outline, while also incorporating the impact of nearby ecosystems, would increase the real-world accuracy of this methodology.



Better city delineation methods could also address the error introduced by the edge effect as discussed in section 5.2.7. Further research into the spatial extent of where pixel error from edge effect is introduced could also help define what kinds of buffer spaces around cities would be necessary to reduce edge effect error while including adjacent ES. Here, the buffer area assigned to a city would need to be large enough that the impact of peri-urban ES can be understood, but that the extent of error from edge effect can be removed from the city extent after landcover classification but before the “Reclass” step. Many improvements to this methodology could be elucidated by a study that focuses more directly on the city extents used in the research.

Furthermore, changes in methods when it comes to the data analysis portion can also be investigated. One shortcoming of this study was that although 500 ground truthing points were completed, those were spread across ten cities, meaning that each city only had fifty ground-truthing points. If future studies focus on fewer cities, this would allow the authors to perform more ground truthing points per city, which could identify additional changes to the methodology that could increase accuracy.

Another useful study could look at how this methodology processes green roofs. None of the ground truthing points landed on a green roof, but it is possible that they could be combined with “Tree Canopy” given their height. Simply testing this model on an area with known green roof locations could clarify this potential source of error.

In terms of usability, the data from this methodology could be more helpful to planners by changing how the final results of the combined ES maps are displayed. For example, in this research, overall ES values were displayed from 0-45. However, this range as a dimensionless unit could be challenging to interpret. For easier interpretation, the combined ES values could be divided by the highest possible value (in this study, 45), and the overall ES value could be a range of 0-1, or a percentage. Those numbers might be easier for non-researchers to understand. The average pixel value of a city or neighborhood could be a percent, which is easier to interpret for policymaking. This way of displaying data could also make future analyses easier to interpret when multiple categories of UES are assessed (i.e. cultural, provisioning, and regulating). So, if the highest possible value for regulating ES is higher than for cultural ES (as there are less categories of cultural ES, so naturally the sum of all cultural



ES could easily be lower than regulating ES), by converting them to percentages, comparisons between ES types would be more intuitive.

The role of local geospatial specialists in contextualizing the data can also be investigated. In the example of the shadows from skyscrapers in Seattle outlined in section 5.2.5, a local expert could look over the data, and spot the inaccurate “Water” pixels in the middle of the dense downtown urban fabric. This would lead to a more accurate overall ES map. However, avoiding specific contextualization by individual analysts was one of the major benefits of a deep learning model for land classification. One possible study could look at avoiding individual analyst intervention until after the landcover classification step. That way, obvious errors could be fixed before ES values are calculated, but individual bias in all the other steps could be avoided.

#### **5.4.2. Broader Research Areas**

Beyond specific methodological changes, there are still growth margins in the field of UES research that could contribute to the development of this study. Ecosystem condition is another major focus of the MAES 4th report. The overall health of the ecosystem plays a major role in the capacity for a given landcover to provide certain ES (Maes et al., 2016). It is likely that the current spatial resolution of aerial data is not high enough to estimate the ecosystem condition, and may require on-site measurements to determine. As methods for defining ecosystem condition of urban ecosystems develop, those guidelines should be incorporated whenever possible to geospatial UES mapping.

With regards to the Service Providing Units in the MAES 4<sup>th</sup> report, many of them can still be challenging to estimate with remotely sensed data or common urban GIS datasets. It can be extremely challenging to use spectral data to determine whether a backyard garden is producing food, which changes estimates of provisioning UES. And when it comes to estimating the insect pollinator ES (see figure 3), there are several challenges. Firstly, because plants flower across the entire growing season, a single spectral snapshot will not have the temporal resolution necessary to identify flowering plants throughout the year. And while 1m resolution is still considered fairly high for remotely sensed data, it is still too coarse for identification of flowering plant cycles. Additionally, the model was not successful at identifying permeable land, which must be prioritized over impervious surfaces when it comes to ES-informed land

use planning. As such, it will be important to track the further development of GIS tools that can identify permeable versus impermeable surfaces on a city-wide scale. For these reasons, there are still several obstacles to a remote sensing methodology that includes all UES outlined in the MAES 4th report. However, as the field progresses, it would be beneficial to include future breakthroughs in UES assessment methodologies.

Finally, as the fields of AI and deep learning continue to develop, it could be beneficial to look at multiple landcover classification models that are trained across a variety of climates. Within this study, all ten of the pilot cities were temperate or arid. The training site for the deep learning model used here, Chesapeake Bay, Vermont, is a temperate coastal environment. This study did not look at any cities in boreal or tropical environments, but it is possible that those could have more error given their large difference in spectral signatures from the training site. For example, epiphytes in tropical areas could cause “Impervious Surfaces” to get categorized as a type of vegetation. And it is unclear how the model would address permafrost or frozen water. Given the wide range of potential spectral signatures across multiple climactic zones, different landcover classification models for different climates could be helpful. They could be broken down by Koppen Climate Classifications, or just overarching climactic zones (e.g. arid, temperate, tropic, and boreal). It is understandable that there is not this diversity of multiclass, high-resolution deep learning models at this time. However, as AI continues to become more integrated in environmental science and GIS, there is possibility for a significant increase in available deep learning models for these applications. And climate zone-specific models could become critical to a deeper understanding of UES on a planetary scale.

## **5.5. Conclusion**

Although this model functioned well for this initial trial in ES evaluation, there is still growth potential in this methodology. The initial CV of the raw data was somewhat high, but after adjusting the data and redoing accuracy assessments, the per-city CV was low enough to accept the results as accurate. The average 88% accuracy is also a strong result for a first study; however, the continued improvements outlined in section 5.4 could push that average even higher. Additionally, the transformation of the overall ES values from a sum to a percent of the highest possible value will increase the usability of the data for policymakers.

Global ES mapping is an important issue, and the spatial heterogeneity and population density of urban environments presents unique challenges to this endeavour. However, the rapidly expanding field of AI and deep learning will offer many new tools for transforming the abundance of raw data into actionable research. Here, an EU-funded UES research project was combined with a deep learning model and the large database of free American data, to streamline the assessment of regulating UES across multiple cities with a unified methodology. Hopefully, we will see many more intersectional studies that decrease the obstacles and costs in UES assessments, thereby increasing the data-driven tools available to policymakers, and supporting the development of ecologically-informed and climate-smart urban planning.



## References

- Andersson-Sköld, Y., Klingberg, J., Gunnarsson, B., Cullinane, K., Gustafsson, I., Hedblom, M., Knez, I., Lindberg, F., Ode Sang, Å., Pleijel, H., Thorsson, P. and Thorsson, S. (2018). A framework for assessing urban greenery's effects and valuing its ecosystem services. *Journal of Environmental Management*, 205, pp.274–285. doi:<https://doi.org/10.1016/j.jenvman.2017.09.071>.
- ArcGIS API for Python (2023). Deep Learning Libraries Installers for ArcGIS. [online] GitHub. Available at: <https://github.com/esri/deep-learning-frameworks> [Accessed 16 Jul. 2023].
- Barbero-Sierra, C., Marques, M.J. and Ruíz-Pérez, M. (2013). The case of urban sprawl in Spain as an active and irreversible driving force for desertification. *Journal of Arid Environments*, 90, pp.95–102. doi:<https://doi.org/10.1016/j.jaridenv.2012.10.014>.
- Bolund, P. and Hunhammar, S. (1999). Ecosystem services in urban areas. *Ecological Economics*, 29(2), pp.293–301. doi:[https://doi.org/10.1016/s0921-8009\(99\)00013-0](https://doi.org/10.1016/s0921-8009(99)00013-0).
- Burkhard, B. and Maes, J. (2017). Mapping Ecosystem Services. Advanced Books, [online] 1, p.e12837. doi:<https://doi.org/10.3897/ab.e12837>.
- C. Daly, G. H. Taylor, W. P. Gibson, T. W. Parzybok, G. L. Johnson and P. A. Pasteris (2000). HIGH-QUALITY SPATIAL CLIMATE DATA SETS FOR THE UNITED STATES AND BEYOND. *Transactions of the ASAE*, 43(6), pp.1957–1962. doi:<https://doi.org/10.13031/2013.3101>.
- Calderón-Argelich, A., Benetti, S., Anguelovski, I., Connolly, J.J.T., Langemeyer, J. and Baró, F. (2021). Tracing and building up environmental justice considerations in the urban ecosystem service literature: A systematic review. *Landscape and Urban Planning*, [online] 214, p.104130. doi:<https://doi.org/10.1016/j.landurbplan.2021.104130>.

Campagne, C.S., Roche, P., Müller, F. and Burkhard, B. (2020). Ten years of ecosystem services matrix: Review of a (r)evolution. *One Ecosystem*, 5. doi:<https://doi.org/10.3897/oneeco.5.e51103>.

Davies, Z.G., Edmondson, J.L., Heinemeyer, A., Leake, J.R. and Gaston, K.J. (2011). Mapping an urban ecosystem service: quantifying above-ground carbon storage at a city-wide scale. *Journal of Applied Ecology*, 48(5), pp.1125–1134. doi:<https://doi.org/10.1111/j.1365-2664.2011.02021.x>.

de Araujo Barbosa, C.C., Atkinson, P.M. and Dearing, J.A. (2015). Remote sensing of ecosystem services: A systematic review. *Ecological Indicators*, 52, pp.430–443. doi:<https://doi.org/10.1016/j.ecolind.2015.01.007>.

Delpy, F., Pedersen Zari, M., Jackson, B., Benavidez, R. and Westend, T. (2021). Ecosystem Services Assessment Tools for Regenerative Urban Design in Oceania. *Sustainability*, 13(5), p.2825. doi:<https://doi.org/10.3390/su13052825>.

Esri (2020). Tree Point Detection. [online] Arcgis.com. Available at: <https://www.arcgis.com/home/item.html?id=58d77b24469d4f30b5f68973deb65599> [Accessed 16 Jul. 2023].

Esri (2023a). High Resolution Land Cover Classification - USA. [online] Arcgis.com. Available at: <https://www.arcgis.com/home/item.html?id=a10f46a8071a4318bcc085dae26d7ee4> [Accessed 16 Jul. 2023].

Esri (2023b). Living Atlas of the World | ArcGIS. [online] [livingatlas.arcgis.com](https://livingatlas.arcgis.com/en/home/). Available at: <https://livingatlas.arcgis.com/en/home/>.

García-Pardo, K.A., Moreno-Rangel, D., Domínguez-Amarillo, S. and García-Chávez, J.R. (2022). Remote sensing for the assessment of ecosystem services provided by urban vegetation: A review of the methods applied. *Urban Forestry & Urban Greening*, 74, p.127636. doi:<https://doi.org/10.1016/j.ufug.2022.127636>.

Grekousis, G. (2019). Artificial neural networks and deep learning in urban geography: A systematic review and meta-analysis. *Computers, Environment and Urban Systems*, 74, pp.244–256. doi:<https://doi.org/10.1016/j.compenvurbsys.2018.10.008>.

Hack, J., Molewijk, D. and Beißler, M.R. (2020). A Conceptual Approach to Modeling the Geospatial Impact of Typical Urban Threats on the Habitat Quality of River Corridors. *Remote Sensing*, 12(8), p.1345. doi:<https://doi.org/10.3390/rs12081345>.

Harrison, P.A., Dunford, R., Barton, D.N., Kelemen, E., Martín-López, B., Norton, L., Termansen, M., Saarikoski, H., Hendriks, K., Gómez-Baggethun, E., Czucz, B., García-Llorente, M., Howard, D., Jacobs, S., Karlsen, M., Kopperoinen, L., Madsen, A., Rusch, G., van Eupen, M. and Verweij, P. (2018). Selecting methods for ecosystem service assessment: A decision tree approach. *Ecosystem Services*, 29, pp.481–498. doi:<https://doi.org/10.1016/j.ecoser.2017.09.016>.

Haske, B., Tanya Brodie Rudolph and Bernsdorf, B. (2021). Sustainability in energy storages - How modern geoscience concepts can improve underground storage monitoring. *International Journal of Earth and Environmental Sciences*. doi:<https://doi.org/10.3997/2214-4609.202121014>.

Konstantinovskiy, L., Price, O., Babakar, M. and Zubiaga, A. (2021). Toward Automated Factchecking. *Digital Threats: Research and Practice*, 2(2), pp.1–16. doi:<https://doi.org/10.1145/3412869>.

Lehmann, I., Mathey, J., Rößler, S., Bräuer, A. and Goldberg, V. (2014). Urban vegetation structure types as a methodological approach for identifying ecosystem services – Application to the analysis of micro-climatic effects. *Ecological Indicators*, [online] 42, pp.58–72. doi:<https://doi.org/10.1016/j.ecolind.2014.02.036>.

Liu, D. and Xia, F. (2010). Assessing object-based classification: advantages and limitations. *Remote Sensing Letters*, 1(4), pp.187–194. doi:<https://doi.org/10.1080/01431161003743173>.

Maes, J., Egoh, B., Willemsen, L., Liqueste, C., Vihervaara, P., Schägner, J.P., Grizzetti, B., Drakou, E.G., Notte, A.L., Zulian, G., Bouraoui, F., Luisa Paracchini, M., Braat, L. and

Bidoglio, G. (2012). Mapping ecosystem services for policy support and decision making in the European Union. *Ecosystem Services*, 1(1), pp.31–39. doi:<https://doi.org/10.1016/j.ecoser.2012.06.004>.

Maes, J., Zulian, G., Thijssen, M., Castell, C. and Teller, A. (2016). Mapping and Assessment of Ecosystems and their Services: Urban ecosystems. Baidu Scholar. [online] doi:<https://doi.org/10.2779/625242>.

Marando, F., Heris, M.P., Zulian, G., Udías, A., Mentaschi, L., Chrysoulakis, N., Parastatidis, D. and Maes, J. (2022). Urban heat island mitigation by green infrastructure in European Functional Urban Areas. *Sustainable Cities and Society*, 77, p.103564. doi:<https://doi.org/10.1016/j.scs.2021.103564>.

Mathey, J., Hennersdorf, J., Lehmann, I. and Wende, W. (2021). Qualifying the urban structure type approach for urban green space analysis – A case study of Dresden, Germany. *Ecological Indicators*, 125, p.107519. doi:<https://doi.org/10.1016/j.ecolind.2021.107519>.

Müller, N., Ignatieva, M., Nilon, C.H., Werner, P. and Zipperer, W.C. (2013). Patterns and Trends in Urban Biodiversity and Landscape Design. *Urbanization, Biodiversity and Ecosystem Services: Challenges and Opportunities*, pp.123–174. doi:[https://doi.org/10.1007/978-94-007-7088-1\\_10](https://doi.org/10.1007/978-94-007-7088-1_10).

Newman, P. (2006). The environmental impact of cities. *Environment and Urbanization*, 18(2), pp.275–295. doi:<https://doi.org/10.1177/0956247806069599>.

Rakoto, P.Y., Deilami, K., Hurley, J., Amati, M. and Sun, Q. (Chayn) (2021). Revisiting the cooling effects of urban greening: Planning implications of vegetation types and spatial configuration. *Urban Forestry & Urban Greening*, 64, p.127266. doi:<https://doi.org/10.1016/j.ufug.2021.127266>.

Sassen, S. (2010). Cities are at the center of our environmental future. *Revista de Ingeniería*, (31), pp.72–83. doi:<https://doi.org/10.16924/revinge.31.8>.



Säumel, I., Weber, F. and Kowarik, I. (2016). Toward livable and healthy urban streets: Roadside vegetation provides ecosystem services where people live and move. *Environmental Science & Policy*, 62, pp.24–33. doi:<https://doi.org/10.1016/j.envsci.2015.11.012>.

Tiner, R.W. (1993). The primary indicators method—A practical approach to wetland recognition and delineation in the United States. *Wetlands*, 13(1), pp.50–64. doi:<https://doi.org/10.1007/bf03160865>.

Trinder, J.C. (2021). Remote Sensing for Ecosystem Services and Urban Sustainability. *Photogrammetric Engineering & Remote Sensing*, 87(3), pp.188–194. doi:<https://doi.org/10.14358/pers.87.3.189>.

U.S. General Services Administration (2020). 500 Cities: City Boundaries. [online] Data.gov. Available at: <https://catalog.data.gov/dataset/500-cities-city-boundaries>.

USGS (2022). Download Data & Maps from The National Map | U.S. Geological Survey. [online] [www.usgs.gov](http://www.usgs.gov). Available at: <https://www.usgs.gov/tools/download-data-maps-national-map> [Accessed 16 Jul. 2023].

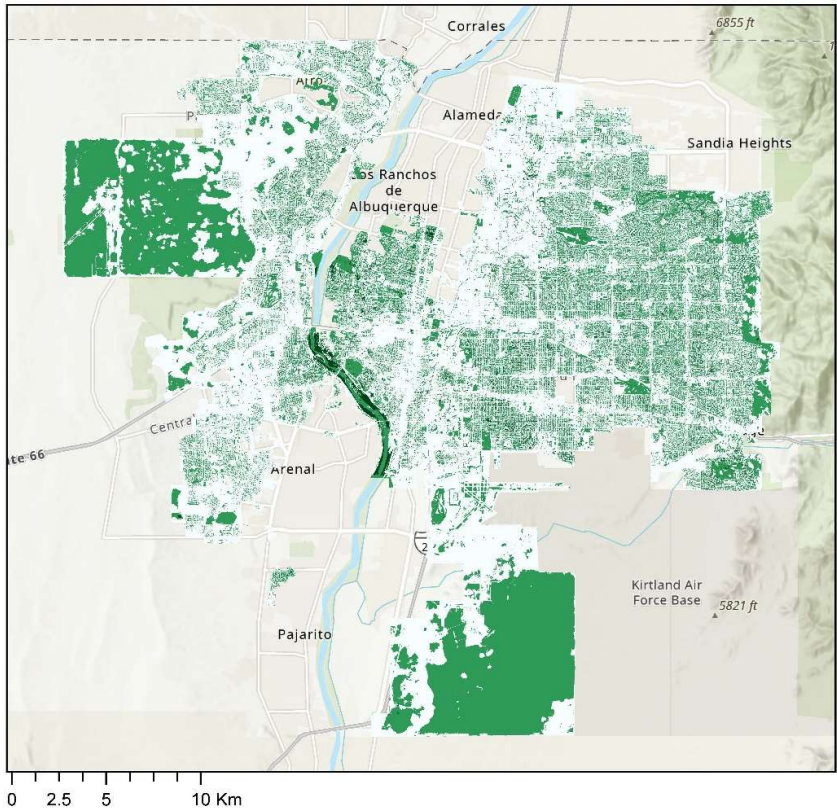
Van Renterghem, T. (2019). Towards explaining the positive effect of vegetation on the perception of environmental noise. *Urban Forestry & Urban Greening*, 40, pp.133–144. doi:<https://doi.org/10.1016/j.ufug.2018.03.007>.

[www.eea.europa.eu](http://www.eea.europa.eu). (2017). Glossary for urban green infrastructure — European Environment Agency. [online] Available at: [https://www.eea.europa.eu/themes/sustainability-transitions/urban-environment/urban-green-infrastructure/glossary-for-urban-green-infrastructure#:~:text=Green%20Infrastructure%20\(GI\)%3A%20A](https://www.eea.europa.eu/themes/sustainability-transitions/urban-environment/urban-green-infrastructure/glossary-for-urban-green-infrastructure#:~:text=Green%20Infrastructure%20(GI)%3A%20A) [Accessed 16 Jul. 2023].

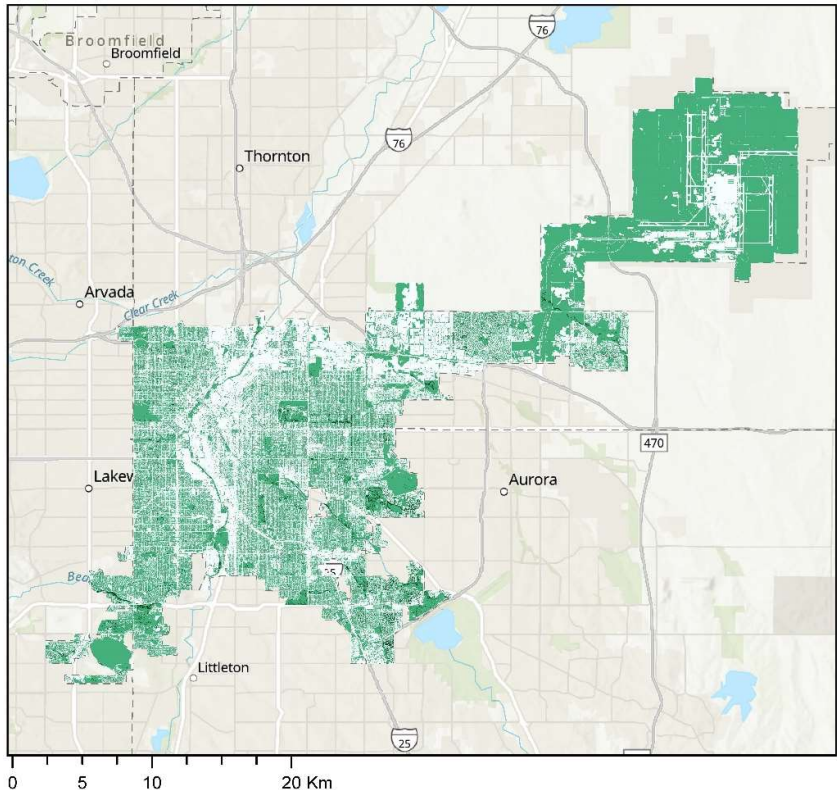


Appendices

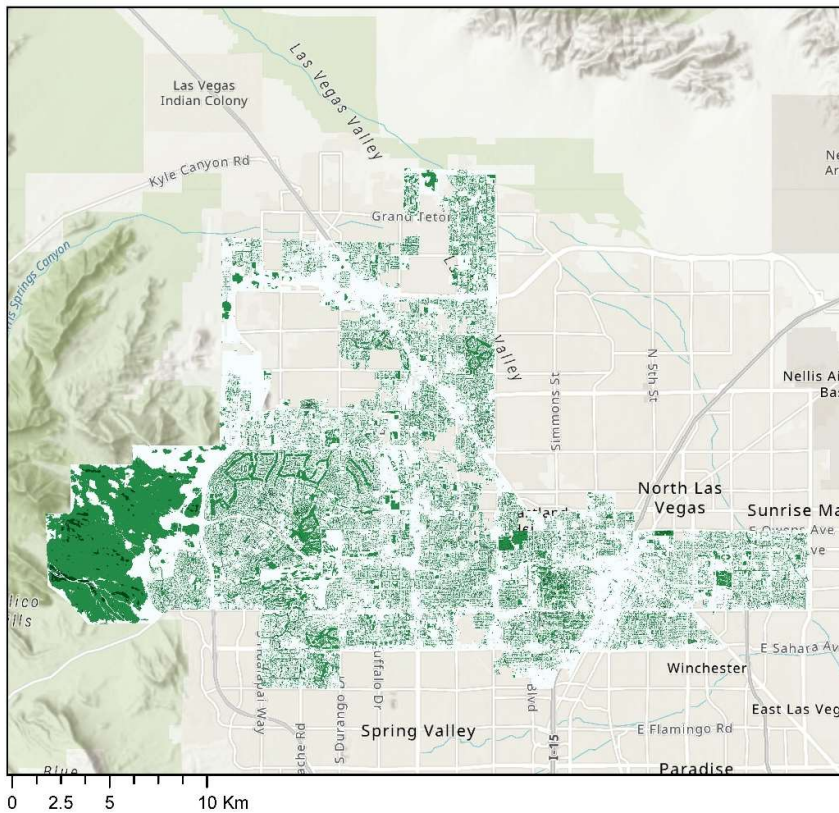
Appendix A: Overall Ecosystem Service Value Maps for Each Pilot City



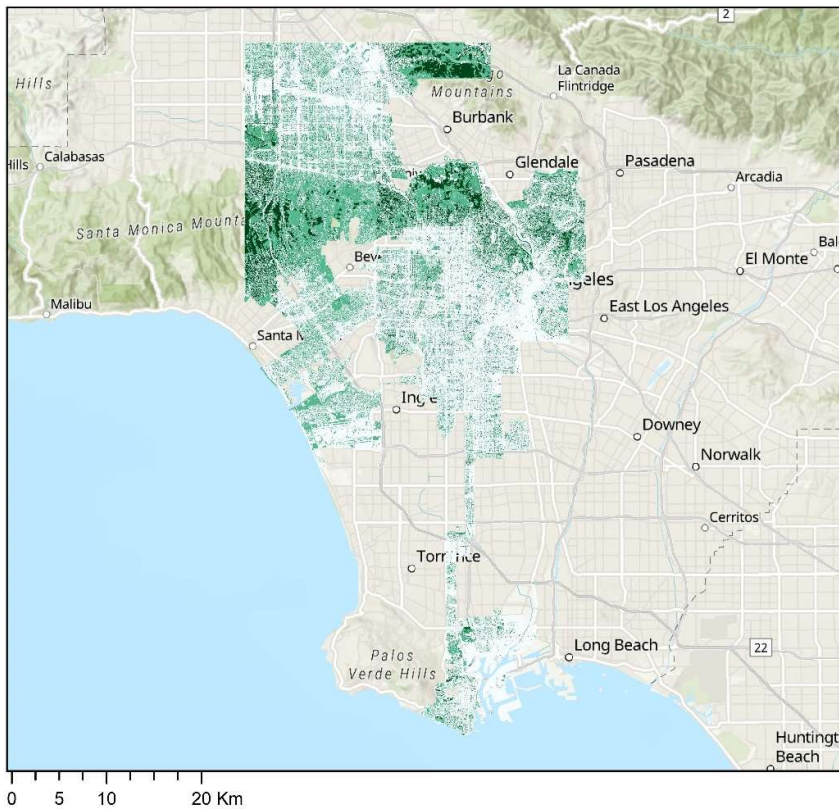
City: Albuquerque, NM  
Mean Pixel Value: 7.68



City: Denver, CO  
Mean Pixel Value: 11.45

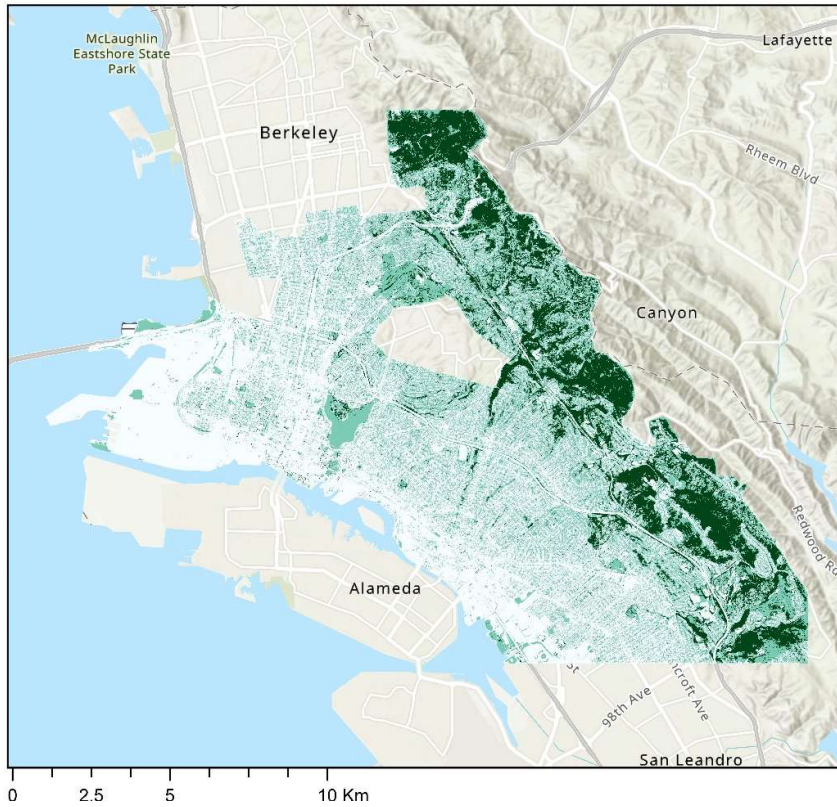


City: Las Vegas, NV  
Mean Pixel Value: 6.42

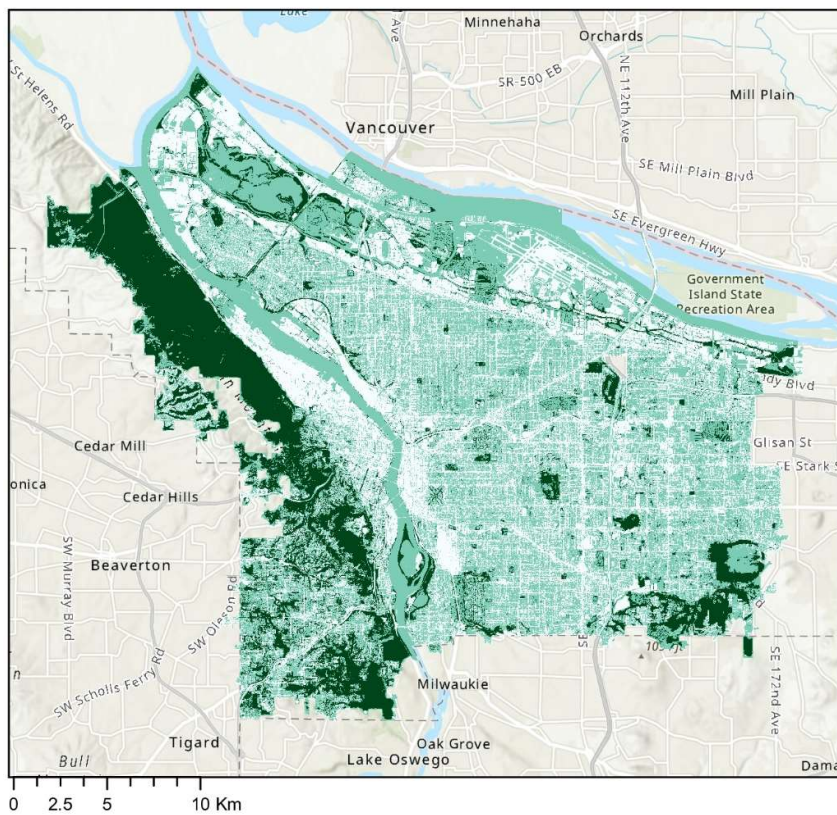


City: Los Angeles, CA  
Mean Pixel Value: 9.52

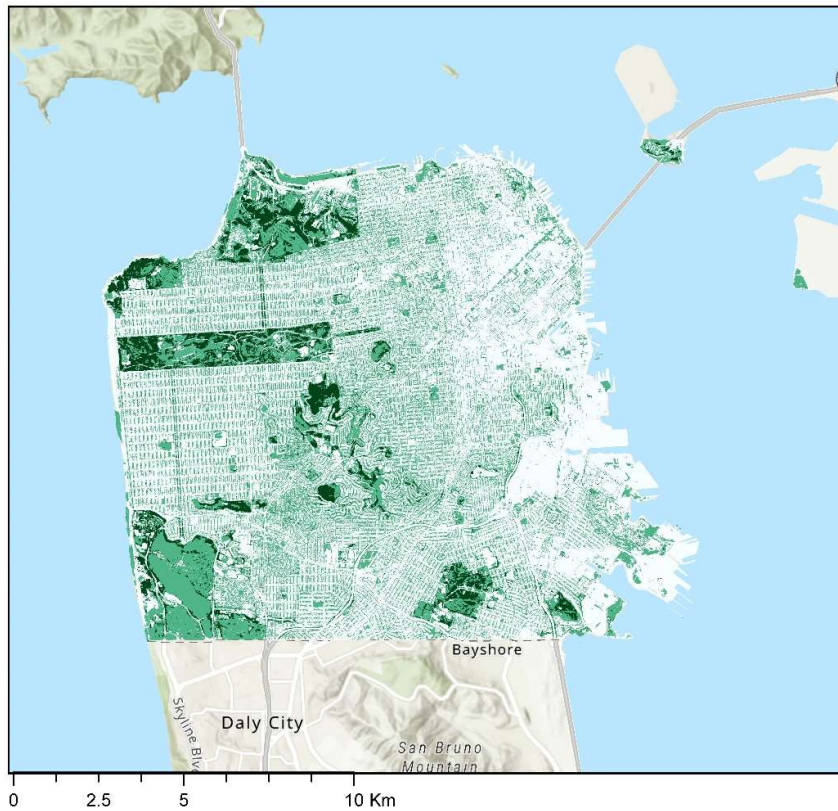




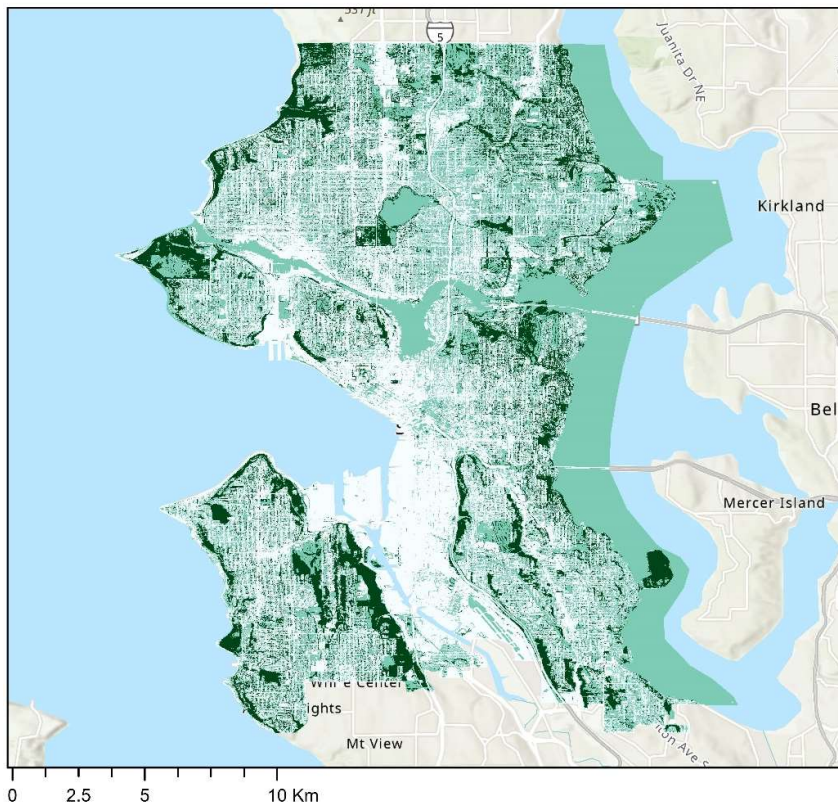
City: Oakland, CA  
Mean Pixel Value: 13.09



City: Portland, OR  
Mean Pixel Value: 17.79

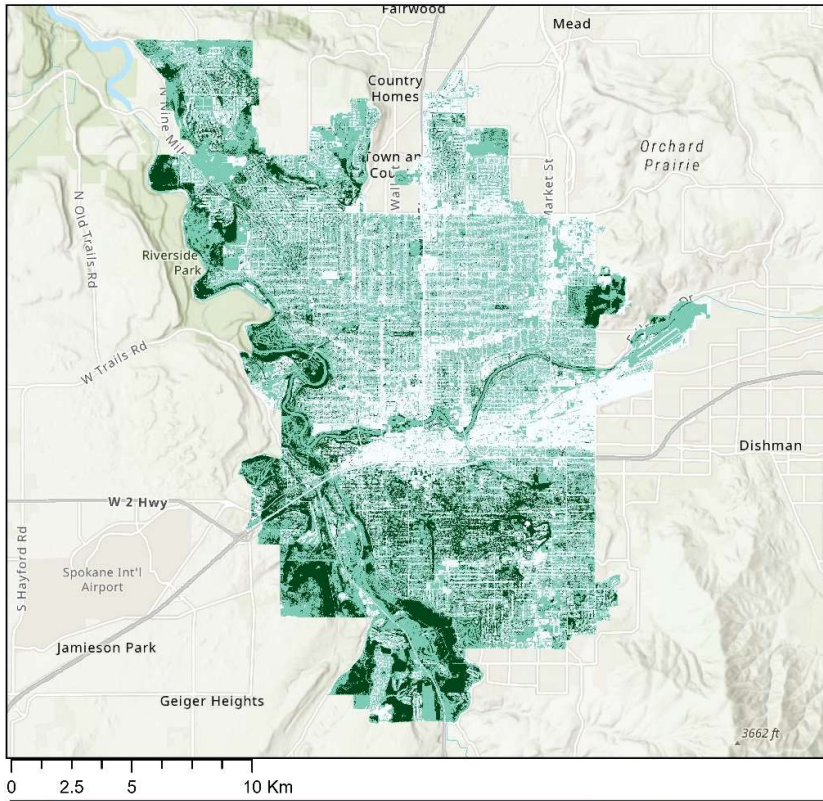


City: San Francisco, CA  
Mean Pixel Value: 8.89

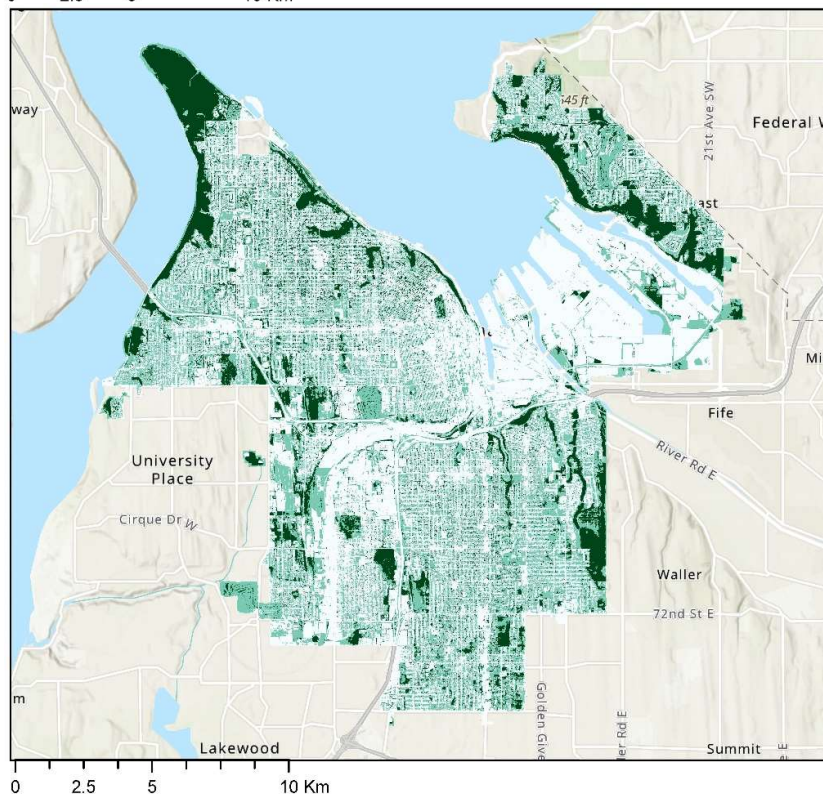


City: Seattle, WA  
Mean Pixel Value: 15.43





City: Spokane, WA  
Mean Pixel Value: 16.64



City: Tacoma, WA  
Mean Pixel Value: 12.97

## Appendix B: Ground Truthing Tables and Calculations

Albuquerque, NM							
X	Y	Classification	Correct	True Class if Incorrect			
35.15614124	-106.7920549	Barren	y		<b>Totals</b>		
35.15649372	-106.7318888	Barren		Low Vegetation	<b>Class</b>	<b># Points</b>	<b># Accurate</b>
35.01496776	-106.5875519	Barren	y		Barren	9	6
35.13726519	-106.7178497	Barren		Low Vegetation	Impervious Roads	2	2
35.01560634	-106.6279015	Barren	y		Impervious Surf.	13	11
34.95625497	-106.576129	Barren	y		Low Vegetation	19	15
35.06132994	-106.6184219	Barren	y		Structures	3	2
35.01920814	-106.6210781	Barren		Impervious Surfaces	Tree Canopy	3	3
34.95247102	-106.5766133	Barren	y		Wetlands	2	1
35.09070746	-106.6633794	Impervious Roads	y		Overall	50	39
35.11473113	-106.6004497	Impervious Roads	y				
35.04312584	-106.6261541	Impervious Surfaces	y		<b>Adjusted Data</b>		
35.09533919	-106.6721093	Impervious Surfaces	y		<b>Class</b>	<b># Points</b>	<b># Accurate</b>
35.04581977	-106.5957349	Impervious Surfaces	y		Trees/Shrubs	3	3
35.19842012	-106.5932513	Impervious Surfaces	y		LV/Wetlands	21	17
35.17542778	-106.786908	Impervious Surfaces		Barren	Water	0	0
35.14665804	-106.5515718	Impervious Surfaces	y		Built/Barren	27	25
35.10510529	-106.5269259	Impervious Surfaces	y		Overall	50	44
35.19686657	-106.5757251	Impervious Surfaces	y				
35.19067642	-106.5568754	Impervious Surfaces	y				
35.12367505	-106.6413844	Impervious Surfaces	y				
35.05705262	-106.6177431	Impervious Surfaces	y				
35.08110801	-106.6135384	Impervious Surfaces		Impervious Roads			
35.09670485	-106.7552032	Impervious Surfaces	y				
35.14598799	-106.5141248	Low Vegetation	y				
35.07334806	-106.5135326	Low Vegetation	y				
35.14863144	-106.6427483	Low Vegetation		Impervious Surfaces			
35.14804776	-106.8029637	Low Vegetation	y				
35.12256998	-106.5728709	Low Vegetation		Structures			
34.98480112	-106.6096971	Low Vegetation	y				
35.15711385	-106.7794657	Low Vegetation	y				
35.10309558	-106.5387308	Low Vegetation	y				
35.12186939	-106.5310088	Low Vegetation	y				
35.17142763	-106.7604253	Low Vegetation	y				
35.02688808	-106.7295023	Low Vegetation	y				
34.96381384	-106.5897664	Low Vegetation	y				
35.13929722	-106.5429241	Low Vegetation		Tree Canopy			
35.09577412	-106.5203413	Low Vegetation	y				
34.96120277	-106.6506409	Low Vegetation	y				
34.99711318	-106.606857	Low Vegetation	y				
35.10091175	-106.5132479	Low Vegetation		Impervious Surfaces			
35.14041514	-106.7130662	Low Vegetation	y				
35.17389351	-106.5854128	Structures		Impervious Surfaces			
35.12754445	-106.5824647	Structures	y				
35.17216635	-106.6932651	Structures	y				
35.04681884	-106.5008175	Tree Canopy	y				
35.08059828	-106.665383	Tree Canopy	y				
35.08948355	-106.5955909	Tree Canopy	y				
35.09840347	-106.479476	Wetlands		Low Vegetation			
35.13586458	-106.8142267	Wetlands	y				



Denver, CO						
X	Y	Classification	Correct ?	True Class if Incorrect		
39.83275875	-104.6674105	Barren		Low Vegetation	<b>Totals</b>	
39.69676807	-104.9926291	Impervious Roads	y		<b>Class</b>	<b># Points # Accurate</b>
39.79078824	-104.9801548	Impervious Surfaces	y		Barren	1 0
39.84185765	-104.7587026	Impervious Surfaces	y		Impervious Roads	1 1
39.76847317	-104.975514	Impervious Surfaces		Structures	Impervious Surf.	9 8
39.82601884	-104.7688782	Impervious Surfaces	y		Low Vegetation	32 25
39.84683409	-104.66813	Impervious Surfaces	y		Structures	2 2
39.73392814	-104.9638695	Impervious Surfaces	y		Tree Canopy	3 3
39.79175237	-104.9423924	Impervious Surfaces	y		Water	2 2
39.8639124	-104.6650171	Impervious Surfaces	y		Overall	50 41
39.7909622	-104.9880688	Impervious Surfaces	y			
39.79008076	-104.7407285	Low Vegetation	y		<b>Adjusted Data</b>	
39.6922826	-104.931035	Low Vegetation		Impervious Surfaces	<b>Class</b>	<b># Points # Accurate</b>
39.69688026	-105.0024891	Low Vegetation	y		Trees/Shrubs	3 3
39.77098398	-104.7444409	Low Vegetation		Impervious Surfaces	LV/Wetlands	32 25
39.8353463	-104.6664282	Low Vegetation	y		Water	2 2
39.75436096	-105.0411703	Low Vegetation		Tree Canopy	Built/Barren	13 12
39.67360906	-104.9464672	Low Vegetation	y		Overall	50 42
39.63120757	-105.0852251	Low Vegetation		Tree Canopy		
39.7809235	-104.7761447	Low Vegetation	y			
39.75220155	-104.9827761	Low Vegetation	y			
39.8465476	-104.6210875	Low Vegetation	y			
39.66799695	-105.032347	Low Vegetation		Tree Canopy		
39.82525808	-104.7016547	Low Vegetation	y			
39.6542911	-104.8976268	Low Vegetation	y			
39.6326032	-104.8887618	Low Vegetation	y			
39.66188376	-105.0210861	Low Vegetation	y			
39.82737963	-104.6503556	Low Vegetation	y			
39.8387557	-104.7632202	Low Vegetation		Baren		
39.69725012	-104.9131522	Low Vegetation	y			
39.86856728	-104.6690728	Low Vegetation	y			
39.87098928	-104.686632	Low Vegetation	y			
39.68038697	-104.9470949	Low Vegetation	y			
39.7723413	-104.7455217	Low Vegetation	y			
39.71968163	-105.0519486	Low Vegetation		Impervious Surfaces		
39.8964832	-104.6491329	Low Vegetation	y			
39.84379368	-104.7581669	Low Vegetation	y			
39.85534743	-104.6857584	Low Vegetation	y			
39.62237014	-105.0569348	Low Vegetation	y			
39.85379035	-104.6862769	Low Vegetation	y			
39.82362927	-104.6834375	Low Vegetation	y			
39.75908235	-105.0287341	Low Vegetation	y			
39.71923055	-105.0059868	Low Vegetation	y			
39.78232194	-104.9306871	Structures	y			
39.71597212	-105.0261466	Structures	y			
39.71038323	-104.9053893	Tree Canopy	y			
39.69847881	-104.9697951	Tree Canopy	y			
39.88329711	-104.6178442	Tree Canopy	y			
39.6321743	-105.0764073	Water	y			
39.63244154	-105.0728711	Water	y			

Las Vegas, NV							
X	Y	Classification	Correct ?	True Class if Incorrect			
36.24537282	-115.3181036	Barren	y		<b>Totals</b>		
36.28154205	-115.2208491	Barren		Impervious Surfaces	<b>Class</b>	<b># Points</b>	<b># Accurate</b>
36.23629243	-115.3260028	Barren		Impervious Surfaces	Barren	4	2
36.15886166	-115.3673939	Barren	y		Impervious Roads	4	4
36.16966661	-115.2591373	Impervious Roads	y		Impervious Surf.	18	18
36.16052029	-115.1419334	Impervious Roads	y		Low Vegetation	8	5
36.20364916	-115.3168788	Impervious Roads	y		Structures	12	11
36.17406905	-115.3541183	Impervious Roads	y		Tree Canopy	3	3
36.15171367	-115.1129754	Impervious Surfaces	y		Wetlands	1	0
36.20313247	-115.2415308	Impervious Surfaces	y		Overall	50	43
36.21332593	-115.2572348	Impervious Surfaces	y				
36.23664413	-115.2520604	Impervious Surfaces	y		<b>Adjusted Data</b>		
36.16247901	-115.1841236	Impervious Surfaces	y		<b>Class</b>	<b># Points</b>	<b># Accurate</b>
36.26591591	-115.2404352	Impervious Surfaces	y		Trees/Shrubs	3	3
36.24587454	-115.2125936	Impervious Surfaces	y		LV/Wetlands	9	6
36.14426867	-115.2596284	Impervious Surfaces	y		Water	0	0
36.26147659	-115.2571495	Impervious Surfaces	y		Built/Barren	38	38
36.16290292	-115.1915493	Impervious Surfaces	y		Overall	50	47
36.1918293	-115.301914	Impervious Surfaces	y				
36.17674889	-115.104071	Impervious Surfaces	y				
36.18584682	-115.2453652	Impervious Surfaces	y				
36.26220728	-115.2511995	Impervious Surfaces	y				
36.2083807	-115.2873891	Impervious Surfaces	y				
36.23315879	-115.2345835	Impervious Surfaces	y				
36.17239702	-115.0659048	Impervious Surfaces	y				
36.19452546	-115.2167484	Impervious Surfaces	y				
36.23341987	-115.264869	Low Vegetation		Tree Canopy			
36.15026673	-115.1983498	Low Vegetation	y				
36.19335844	-115.1481618	Low Vegetation	y				
36.18905511	-115.377368	Low Vegetation	y				
36.22623008	-115.2123215	Low Vegetation		Barren			
36.153276	-115.1991134	Low Vegetation		Impervious Surfaces			
36.18801683	-115.3001752	Low Vegetation	y				
36.18705962	-115.3651055	Low Vegetation	y				
36.25145226	-115.2078055	Structures	y				
36.18397421	-115.163472	Structures		Impervious Surfaces			
36.17474984	-115.1650708	Structures	y				
36.19754347	-115.3078527	Structures	y				
36.17464324	-115.3485539	Structures	y				
36.1696139	-115.2327117	Structures	y				
36.1570415	-115.1303664	Structures	y				
36.19045511	-115.1491188	Structures	y				
36.18244062	-115.3229374	Structures	y				
36.23486216	-115.3213629	Structures	y				
36.1877749	-115.2523013	Structures	y				
36.15706767	-115.2340944	Structures	y				
36.19734769	-115.2323319	Tree Canopy	y				
36.2726518	-115.2443489	Tree Canopy	y				
36.2001925	-115.3069714	Tree Canopy	y				
36.18565206	-115.4085247	Wetland		Low Vegetation			

Los Angeles, CA							
X	Y	Classification	Correct ?	True Class if Incorrect			
34.1505355	-118.3008345	Barren		Low Vegetation	<b>Totals</b>		
33.97992804	-118.4243272	Barren		Impervious Surfaces	<b>Class</b>	<b># Points</b>	<b># Accurate</b>
34.1647784	-118.3909305	Impervious Surfaces	y		Barren	2	0
33.72290212	-118.3104121	Impervious Surfaces	y		Impervious Roads	0	0
33.92127026	-118.2831772	Impervious Surfaces	y		Impervious Surf.	15	14
33.74844043	-118.2670004	Impervious Surfaces	y		Low Vegetation	11	9
34.15992524	-118.4868625	Impervious Surfaces	y		Structures	15	14
34.02446812	-118.2735005	Impervious Surfaces	y		Tree Canopy	5	5
33.77711198	-118.2757971	Impervious Surfaces	y		Wetlands	2	0
34.13675369	-118.2736105	Impervious Surfaces	y		Overall	50	41
34.23596189	-118.3795234	Impervious Surfaces	y				
33.72176998	-118.2513832	Impervious Surfaces	y		<b>Adjusted Data</b>		
34.02601646	-118.2075249	Impervious Surfaces		Impervious Roads	<b>Class</b>	<b># Points</b>	<b># Accurate</b>
33.99856963	-118.461863	Impervious Surfaces	y		Trees/Shrubs	5	5
34.03130347	-118.3179106	Impervious Surfaces	y		LV/Wetlands	13	11
34.22036133	-118.3626389	Impervious Surfaces	y		Water	0	0
33.79519198	-118.2284358	Impervious Surfaces	y		Built/Barren	32	30
34.10778702	-118.4610618	Low Vegetation		Impervious Surfaces	Overall	50	46
33.79677527	-118.2714097	Low Vegetation	y				
34.2178982	-118.3451158	Low Vegetation	y				
34.10637094	-118.2266306	Low Vegetation	y				
34.03505031	-118.4274622	Low Vegetation		Tree Canopy			
34.21965606	-118.4605609	Low Vegetation	y				
34.12743857	-118.1932077	Low Vegetation	y				
34.05732187	-118.3440549	Low Vegetation	y				
34.16112894	-118.4256081	Low Vegetation		Tree Canopy			
34.14508542	-118.4320424	Low Vegetation	y				
34.19161002	-118.4120805	Low Vegetation	y				
34.10145656	-118.2864043	Structures	y				
34.02328585	-118.4348946	Structures	y				
34.06730948	-118.4436796	Structures	y				
33.9870446	-118.4031586	Structures	y				
34.13058999	-118.485407	Structures	y				
34.06898478	-118.2050028	Structures		Tree Canopy			
34.14288923	-118.4003064	Structures	y				
33.83428117	-118.3062279	Structures	y				
33.99985414	-118.2829054	Structures	y				
34.03657006	-118.340349	Structures	y				
34.10338307	-118.3406593	Structures	y				
34.15535586	-118.3957016	Structures	y				
34.11254314	-118.2681691	Structures	y				
34.06398081	-118.3032921	Structures	y				
34.2449296	-118.3647394	Structures	y				
33.99523377	-118.2501906	Tree Canopy	y				
34.07218314	-118.2026201	Tree Canopy	y				
34.08499056	-118.3405959	Tree Canopy	y				
33.73306077	-118.3160025	Tree Canopy	y				
34.01338179	-118.2830505	Tree Canopy	y				
34.23507625	-118.3218358	Wetlands		Low Vegetation			
34.1007525	-118.420798	Wetlands		Low Vegetation			

Oakland, CA							
X	Y	Classification	Correct ?	True Class if Incorrect			
37.75290058	-122.1581443	Impervious Roads	y		<b>Totals</b>		
37.76571041	-122.1941235	Impervious Roads	y		<b>Class</b>	<b># Points</b>	<b># Accurate</b>
37.8105189	-122.2380164	Impervious Roads	y		Barren	0	0
37.80288835	-122.2536714	Impervious Roads	y		Impervious Roads	4	4
37.75116404	-122.1585189	Impervious Surfaces	y		Impervious Surf.	13	10
37.8461761	-122.2587185	Impervious Surfaces	y		Low Vegetation	8	4
37.77408068	-122.207606	Impervious Surfaces		Impervious Roads	Structures	13	13
37.81036886	-122.1950098	Impervious Surfaces		Impervious Roads	Tree Canopy	11	11
37.82746272	-122.1993514	Impervious Surfaces	y		Water	1	1
37.81898811	-122.2611852	Impervious Surfaces	y		Overall	50	43
37.79746579	-122.2665486	Impervious Surfaces		Impervious Roads			
37.83675559	-122.2075073	Impervious Surfaces	y		<b>Adjusted Data</b>		
37.81914618	-122.2529021	Impervious Surfaces	y		<b>Class</b>	<b># Points</b>	<b># Accurate</b>
37.81077826	-122.2896742	Impervious Surfaces	y		Trees/Shrubs	11	11
37.80652821	-122.2487277	Impervious Surfaces	y		LV/Wetlands	8	4
37.75662338	-122.1638416	Impervious Surfaces	y		Water	1	1
37.76680068	-122.1380833	Impervious Surfaces	y		Built/Barren	30	30
37.79581529	-122.2398543	Low Vegetation	y		Overall	50	46
37.82547082	-122.25017	Low Vegetation	y				
37.8354529	-122.2354788	Low vegetation	y				
37.82919561	-122.2231123	Low Vegetation	y				
37.7648511	-122.1938408	Low Vegetation		Impervious Surfaces			
37.8383565	-122.2030073	Low Vegetation		Tree Canopy			
37.76566896	-122.2073107	Low Vegetation		Tree Canopy			
37.79065614	-122.2403367	Low Vegetation		Tree Canopy			
37.80844788	-122.2206115	Structures	y				
37.82798599	-122.2450711	Structures	y				
37.78220619	-122.2333842	Structures	y				
37.80477406	-122.2203831	Structures	y				
37.79180595	-122.2186447	Structures	y				
37.84770671	-122.2603876	Structures	y				
37.816078	-122.3086648	Structures	y				
37.75355641	-122.1910276	Structures	y				
37.77307612	-122.2192505	Structures	y				
37.75601401	-122.1662024	Structures	y				
37.78529342	-122.2128489	Structures	y				
37.79448988	-122.2103808	Structures	y				
37.82481637	-122.2836623	Structures	y				
37.81513559	-122.200023	Tree Canopy	y				
37.87412189	-122.2245825	Tree Canopy	y				
37.78113329	-122.1836094	Tree Canopy	y				
37.78684918	-122.1595411	Tree Canopy	y				
37.81276074	-122.1752423	Tree Canopy	y				
37.81685654	-122.1928347	Tree Canopy	y				
37.81374877	-122.2070309	Tree Canopy	y				
37.79211632	-122.1769161	Tree Canopy	y				
37.81545144	-122.1943816	Tree Canopy	y				
37.76589495	-122.1398358	Tree Canopy	y				
37.81675288	-122.1980447	Tree Canopy	y				
37.80167815	-122.2568213	Water	y				

Portland, OR							
X	Y	Classification	Correct ?	True Class if Incorrect			
-122.6735316	45.53129824	Barren		Impervious Surfaces	<b>Totals</b>		
-122.5971052	45.47680452	Impervious Roads	y		<b>Class</b>	<b># Points</b>	<b># Accurate</b>
-122.7159086	45.4674483	Impervious Roads	y		Barren	1	0
-122.5803009	45.50793382	Impervious Surfaces	y		Impervious Roads	2	2
-122.7755981	45.63756615	Impervious Surfaces	y		Impervious Surf.	6	6
-122.555696	45.5705838	Impervious Surfaces	y		Low Vegetation	15	10
-122.7061721	45.614345	Impervious Surfaces	y		Structures	9	9
-122.5581566	45.51859149	Impervious Surfaces	y		Tree Canopy	13	13
-122.7569014	45.63688225	Impervious Surfaces	y		Water	4	3
-122.5812133	45.48910671	Low Vegetation	y		Overall	50	43
-122.6039742	45.58875521	Low Vegetation	y				
-122.6719781	45.4618131	Low Vegetation		Tree Canopy	<b>Adjusted Data</b>		
-122.6627392	45.48139133	Low Vegetation	y		<b>Class</b>	<b># Points</b>	<b># Accurate</b>
-122.6734853	45.55439436	Low Vegetation	y		Trees/Shrubs	13	13
-122.5983511	45.49240583	Low Vegetation		Tree Canopy	LV/Wetlands	15	10
-122.7464536	45.61231507	Low Vegetation	y		Water	4	3
-122.4996485	45.55652498	Low Vegetation	y		Built/Barren	18	18
-122.5379115	45.49301662	Low Vegetation	y		Overall	50	44
-122.6872622	45.5671505	Low Vegetation	y				
-122.6104051	45.53872935	Low Vegetation		Tree Canopy			
-122.627682	45.57874492	Low Vegetation	y				
-122.756873	45.60032179	Low Vegetation	y				
-122.503409	45.54159138	Low Vegetation		Tree Canopy			
-122.5225992	45.46141581	Low Vegetation		Tree Canopy			
-122.6448636	45.4825512	Structures	y				
-122.6275856	45.47034708	Structures	y				
-122.4914949	45.55322536	Structures	y				
-122.540085	45.51368548	Structures	y				
-122.6732807	45.48816971	Structures	y				
-122.6369823	45.49447663	Structures	y				
-122.5782715	45.513484	Structures	y				
-122.6066473	45.5232281	Structures	y				
-122.7607878	45.58955284	Structures	y				
-122.6863167	45.46996951	Tree Canopy	y				
-122.7938206	45.59748382	Tree Canopy	y				
-122.5089969	45.47572458	Tree Canopy	y				
-122.6553248	45.4904958	Tree Canopy	y				
-122.7660205	45.57665232	Tree Canopy	y				
-122.6754378	45.43962353	Tree Canopy	y				
-122.6883801	45.48931808	Tree Canopy	y				
-122.6668466	45.45141246	Tree Canopy	y				
-122.5746154	45.57419667	Tree Canopy	y				
-122.5240668	45.52931487	Tree Canopy	y				
-122.7613655	45.59244159	Tree Canopy	y				
-122.575153	45.56941492	Tree Canopy	y				
-122.6921591	45.52803193	Tree Canopy	y				
-122.623215	45.60835347	Water	y				
-122.7196767	45.61051446	Water	y				
-122.7461183	45.61984122	Water	y				
-122.6753651	45.43571244	Water		Tree Canopy			

San Francisco, CA						
X	Y	Classification	Correct ?	True Class if Incorrect		
37.73897176	-122.5071674	Impervious Roads	y		<b>Totals</b>	
37.73618107	-122.5046509	Impervious Roads	y		<b>Class</b>	<b># Points # Accurate</b>
37.74089031	-122.3770759	Impervious Surfaces	y		Barren	0 0
37.75604526	-122.4136525	Impervious Surfaces		Structures	Impervious Roads	2 2
37.71233849	-122.4537031	Impervious Surfaces		Impervious Roads	Impervious Surf.	16 11
37.72648982	-122.4237996	Impervious Surfaces		Impervious Roads	Low Vegetation	16 12
37.75640317	-122.4992304	Impervious Surfaces		Impervious Roads	Structures	13 13
37.74928958	-122.3774444	Impervious Surfaces	y		Tree Canopy	2 2
37.73405871	-122.3995627	Impervious Surfaces	y		Water	1 0
37.77592197	-122.4847973	Impervious Surfaces	y		Overall	50 40
37.75079254	-122.4965068	Impervious Surfaces	y			
37.74655779	-122.453603	Impervious Surfaces	y		<b>Adjusted Data</b>	
37.71069526	-122.386026	Impervious Surfaces	y		<b>Class</b>	<b># Points # Accurate</b>
37.75956049	-122.3814334	Impervious Surfaces	y		Trees/Shrubs	2 2
37.76598196	-122.5109402	Impervious Surfaces		Barren	LV/Wetlands	16 12
37.7793894	-122.4825844	Impervious Surfaces	y		Water	1 0
37.71446664	-122.4330629	Impervious Surfaces	y		Built/Barren	31 26
37.78434119	-122.4085206	Impervious Surfaces	y		Overall	50 40
37.73109849	-122.3745742	Low Vegetation	y			
37.73335307	-122.5012715	Low Vegetation	y			
37.78891025	-122.4722436	Low Vegetation	y			
37.71282461	-122.4335085	Low Vegetation		Impervious Surfaces		
37.78121226	-122.4654298	Low Vegetation		Impervious Roads		
37.7195672	-122.449009	Low Vegetation		Structures		
37.73672228	-122.3955115	Low Vegetation	y			
37.71277637	-122.4953289	Low Vegetation	y			
37.71088847	-122.4794806	Low Vegetation	y			
37.76899314	-122.4691187	Low Vegetation	y			
37.75607604	-122.3945451	Low Vegetation	y			
37.76879156	-122.3917695	Low Vegetation	y			
37.73035297	-122.3691425	Low Vegetation	y			
37.71287457	-122.5013519	Low Vegetation	y			
37.76607714	-122.4674878	Low Vegetation		Impervious Surfaces		
37.76085746	-122.4448136	Low Vegetation	y			
37.75204671	-122.439668	Structures	y			
37.75148799	-122.4293463	Structures	y			
37.73954549	-122.4462501	Structures	y			
37.77727109	-122.493328	Structures	y			
37.73658873	-122.4275436	Structures	y			
37.76350172	-122.4426014	Structures	y			
37.71113226	-122.44314	Structures	y			
37.72872511	-122.4151897	Structures	y			
37.74432952	-122.4959777	Structures	y			
37.71113161	-122.3995073	Structures	y			
37.7438597	-122.4345166	Structures	y			
37.73907047	-122.5052147	Structures	y			
37.78969352	-122.3854156	Structures	y			
37.75094904	-122.4569704	Tree Canopy	y			
37.76143451	-122.5075772	Tree Canopy	y			
37.73077048	-122.4171277	Water		Low Vegetation		

Seattle, WA							
X	Y	Classification	Correct ?	True Class if Incorrect			
47.54387204	-122.3089199	Barren		Impervious	<b>Totals</b>		
47.66140952	-122.3398596	Impervious Roads	y		<b>Class</b>	<b># Points</b>	<b># Accurate</b>
47.56941691	-122.4038145	Impervious Roads	y		Barren	1	0
47.62322091	-122.3318175	Impervious Surfaces	y		Impervious Roads	2	2
47.56825372	-122.3602629	Impervious Surfaces	y		Impervious Surf.	7	4
47.49574754	-122.2644515	Impervious Surfaces		Low Vegetation	Low Vegetation	16	11
47.51970416	-122.3569875	Impervious Surfaces	y		Structures	10	10
47.62540576	-122.3396307	Impervious Surfaces		Impervious Roads	Tree Canopy	8	8
47.61313885	-122.3453973	Impervious Surfaces		Structures	Water	6	5
47.67654813	-122.3207165	Impervious Surfaces	y		Overall	50	40
47.70191307	-122.3003109	Low Vegetation	y				
47.57752362	-122.3841093	Low Vegetation	y		<b>Adjusted Data</b>		
47.50488657	-122.3769198	Low Vegetation	y		<b>Class</b>	<b># Points</b>	<b># Accurate</b>
47.7086921	-122.3076518	Low Vegetation	y		Trees/Shrubs	8	8
47.56994197	-122.3166415	Low Vegetation	y		LV/Wetlands	16	11
47.52991374	-122.3762343	Low Vegetation		Tree Canopy	Water	6	5
47.66789022	-122.3627129	Low Vegetation		Tree Canopy	Built/Barren	20	19
47.5450829	-122.3732837	Low Vegetation	y		Overall	50	43
47.63567075	-122.4054681	Low Vegetation	y				
47.72447644	-122.2859395	Low Vegetation	y				
47.64700386	-122.3047345	Low Vegetation		Impervious Surfaces			
47.68469125	-122.3928575	Low Vegetation	y				
47.62071781	-122.3105262	Low Vegetation	y				
47.63370444	-122.292273	Low Vegetation	y				
47.67356299	-122.3042942	Low Vegetation		Tree Canopy			
47.61003942	-122.2913821	Low Vegetation		Impervious Surfaces			
47.67617513	-122.2960639	Structures	y				
47.54989819	-122.3889261	Structures	y				
47.59427913	-122.3004078	Structures	y				
47.57636974	-122.3362411	Structures	y				
47.57474829	-122.3876086	Structures	y				
47.73099767	-122.3447816	Structures	y				
47.72351949	-122.3353345	Structures	y				
47.56319481	-122.29434	Structures	y				
47.59951174	-122.3074192	Structures	y				
47.64792441	-122.3526624	Structures	y				
47.56642938	-122.2906092	Tree Canopy	y				
47.69505613	-122.2886213	Tree Canopy	y				
47.66629653	-122.4155096	Tree Canopy	y				
47.62582401	-122.2831573	Tree Canopy	y				
47.63534762	-122.3115441	Tree Canopy	y				
47.65228229	-122.3060867	Tree Canopy	y				
47.53136516	-122.3534633	Tree Canopy	y				
47.66176503	-122.416673	Tree Canopy	y				
47.64850242	-122.3115189	Water	y				
47.66112789	-122.2399284	Water	y				
47.55495164	-122.259126	Water	y				
47.6171004	-122.3289734	Water		Impervious Surfaces			
47.66209636	-122.2356837	Water	y				
47.70858016	-122.2753318	Water	y				



Spokane, WA							
X	Y	Classification	Correct ?	True Class if Incorrect			
47.71623858	-117.4545639	Impervious Roads	y		<b>Totals</b>		
47.62109452	-117.3656625	Impervious Surfaces	y		<b>Class</b>	<b># Points</b>	<b># Accurate</b>
47.71643419	-117.3875862	Impervious Surfaces	y		Barren	0	0
47.65671166	-117.3799054	Impervious Surfaces	y		Impervious Roads	1	1
47.69987434	-117.3360516	Impervious Surfaces		Low Vegetation	Impervious Surf.	11	10
47.64954526	-117.4538804	Impervious Surfaces	y		Low Vegetation	17	11
47.60972876	-117.3467452	Impervious Surfaces	y		Structures	7	7
47.74481471	-117.394303	Impervious Surfaces	y		Tree Canopy	11	11
47.62586735	-117.4023438	Impervious Surfaces	y		Water	3	3
47.71468644	-117.445871	Impervious Surfaces	y		Overall	50	43
47.65317381	-117.3610091	Impervious Surfaces	y				
47.70511571	-117.4677119	Impervious Surfaces	y		<b>Adjusted Data</b>		
47.71482338	-117.4900307	Low Vegetation	y		<b>Class</b>	<b># Points</b>	<b># Accurate</b>
47.65512735	-117.3788665	Low Vegetation		Impervious Surfaces	Trees/Shrubs	11	11
47.62959069	-117.4560376	Low Vegetation	y		LV/Wetlands	17	11
47.68539337	-117.3964277	Low Vegetation	y		Water	3	3
47.67611573	-117.3987782	Low Vegetation		Tree Canopy	Built/Barren	19	18
47.64876714	-117.4293006	Low Vegetation		Tree Canopy	Overall	50	43
47.73795091	-117.50132	Low Vegetation	y				
47.67252563	-117.3782892	Low Vegetation		Impervious Surfaces			
47.60760904	-117.3725256	Low Vegetation	y				
47.6509282	-117.415229	Low Vegetation		Barren			
47.64381841	-117.4317012	Low Vegetation		Tree Canopy			
47.63705931	-117.4108858	Low Vegetation	y				
47.70653229	-117.4322771	Low Vegetation	y				
47.61379507	-117.3650975	Low Vegetation	y				
47.63171104	-117.4192346	Low Vegetation	y				
47.68785175	-117.3919645	Low Vegetation	y				
47.65406833	-117.4501788	Low Vegetation	y				
47.68985427	-117.4046413	Structures	y				
47.67541244	-117.4107185	Structures	y				
47.70249512	-117.3754124	Structures	y				
47.6527209	-117.3983208	Structures	y				
47.6652143	-117.3986137	Structures	y				
47.71443907	-117.4042878	Structures	y				
47.69630157	-117.4039357	Structures	y				
47.73181007	-117.4876921	Tree Canopy	y				
47.60694361	-117.4026005	Tree Canopy	y				
47.62284755	-117.4364407	Tree Canopy	y				
47.72040522	-117.4390736	Tree Canopy	y				
47.63445775	-117.4165826	Tree Canopy	y				
47.62224204	-117.4030938	Tree Canopy	y				
47.69143887	-117.3497356	Tree Canopy	y				
47.64482606	-117.367093	Tree Canopy	y				
47.64885856	-117.46412	Tree Canopy	y				
47.69601613	-117.4957554	Tree Canopy	y				
47.61446126	-117.3555356	Tree Canopy	y				
47.67619566	-117.3436243	Water	y				
47.68262293	-117.3304119	Water	y				
47.68640212	-117.3236159	Water	y				



Tacoma, WA							
X	Y	Classification	Correct ?	True Class if Incorrect			
47.29707289	-122.501417	Barren		Structures	<b>Totals</b>		
47.29858724	-122.5282183	Barren	y		<b>Class</b>	<b># Points</b>	<b># Accurate</b>
47.2692471	-122.3691806	Barren		Impervious Surfaces	Barren	3	1
47.24879789	-122.4351745	Impervious Roads	y		Impervious Roads	4	4
47.19295576	-122.4627152	Impervious Roads	y		Impervious Surf.	16	14
47.20010914	-122.4360046	Impervious Roads	y		Low Vegetation	15	12
47.22755523	-122.4578495	Impervious Roads	y		Structures	6	5
47.23406155	-122.4576587	Impervious Surfaces	y		Tree Canopy	6	5
47.19274948	-122.5110267	Impervious Surfaces		Structures	Water	0	0
47.26541874	-122.397466	Impervious Surfaces	y		Overall	50	41
47.21024787	-122.4478554	Impervious Surfaces	y				
47.24286812	-122.4006073	Impervious Surfaces	y		<b>Adjusted Data</b>		
47.26615833	-122.4080727	Impervious Surfaces	y		<b>Class</b>	<b># Points</b>	<b># Accurate</b>
47.26614064	-122.5171562	Impervious Surfaces	y		Trees/Shrubs	6	5
47.28182894	-122.4797302	Impervious Surfaces	y		LV/Wetlands	15	12
47.24068262	-122.5466978	Impervious Surfaces		Tree Canopy	Water	0	0
47.19611154	-122.450175	Impervious Surfaces	y		Built/Barren	29	27
47.27967321	-122.3916166	Impervious Surfaces	y		Overall	50	44
47.2902735	-122.4005839	Impervious Surfaces	y				
47.21623815	-122.5042986	Impervious Surfaces	y				
47.17747065	-122.4420937	Impervious Surfaces	y				
47.26846948	-122.5137284	Impervious Surfaces	y				
47.22328884	-122.4536904	Impervious Surfaces	y				
47.29576318	-122.3915279	Low Vegetation	y				
47.26793851	-122.4820528	Low Vegetation	y				
47.26958309	-122.4560945	Low Vegetation		Structures			
47.22564155	-122.4167269	Low Vegetation	y				
47.24927756	-122.5286571	Low Vegetation	y				
47.26536362	-122.4622653	Low Vegetation		Tree Canopy			
47.23622981	-122.4586941	Low Vegetation	y				
47.30611205	-122.4098355	Low Vegetation	y				
47.26634727	-122.4969099	Low Vegetation	y				
47.18435922	-122.4300592	Low Vegetation	y				
47.2410819	-122.4037224	Low Vegetation		Tree Canopy			
47.26008471	-122.4735308	Low Vegetation	y				
47.20617165	-122.4241607	Low Vegetation	y				
47.19967511	-122.4165351	Low Vegetation	y				
47.27828483	-122.5181151	Low Vegetation	y				
47.20441909	-122.4886921	Structures	y				
47.20410865	-122.4179656	Structures	y				
47.19811485	-122.4305386	Structures	y				
47.25545111	-122.4475476	Structures		Tree Canopy			
47.25474034	-122.4054117	Structures	y				
47.21601426	-122.4667458	Structures	y				
47.28303844	-122.526389	Tree Canopy	y				
47.18185836	-122.4389054	Tree Canopy	y				
47.19875562	-122.4554296	Tree Canopy	y				
47.26218268	-122.4786546	Tree Canopy		Impervious Surfaces			
47.30537433	-122.4288097	Tree Canopy	y				
47.31246197	-122.5360386	Tree Canopy	y				

## Confusion Matrices

### Raw Data

Actual Classes	Predicted Classes							
	Barren	Imperv. Roads	Imperv. Surfaces	Low Veg.	Structure	Tree Canopy	Water	Wetlands
	Barren	9	2	3				
	Imperv. Roads		22	9	1			
	Imperv. Surfaces	7		106	14	2	1	
	Low Veg.	4		2	114		1	4
	Structure	1		3	3	86		
	Tree Canopy			1	23	2	64	1
	Water						14	
	Wetlands							1

### Adjusted Data

		Predicted Classes			
		Trees/ Shrubs	Low Veg/ Wetlands	Water	Built/ Barren
Actual Classes	Trees/ Shrubs	64	23	1	3
	Ground Veg/ Wetlands		119	1	6
	Water			14	
	Built/ Barren	1	21	1	248

## F1 Scores

### F1 Scores For Raw Data

Classification	ESRI/ USDA	F1 from Study
Barren	0.58	0.51
Impervious Roads	0.79	0.81
Impervious Surfaces	0.71	0.86
Low Vegetation	0.86	0.81
Structures	0.82	0.94
Tree Canopy	0.92	0.82
Water	0.93	0.9
Wetlands	0.79	0.33

### F1 Scores for Adjusted Data

Classification	F1 Score
Trees/Shrubs	0.82
Ground Veg/ Wetlands	0.82
Water	0.9
Built/Barren	0.94

## City Data

City	Accuracy of raw data
Portland	86%
San Francisco	80%
Spokane	86%
Tacoma	82%
Oakland	86%
Los Angeles	82%
Las Vegas	86%
Denver	82%
Albuquerque	82%
Seattle	80%
Average	83.20%
Std. Dev	2.52982

City	Accuracy of adjusted data
Portland	88%
San Francisco	80%
Spokane	86%
Tacoma	88%
Oakland	92%
Los Angeles	92%
Las Vegas	94%
Denver	84%
Albuquerque	88%
Seattle	86%
Average	87.80%
Std Dev	4.15799

### City Combined ES Per-Pixel Averages

City	Per-Pixel Mean
Portland	17.79
San Francisco	8.89
Spokane	16.64
Tacoma	12.97
Oakland	13.09
Los Angeles	9.52
Las Vegas	6.42
Denver	11.45
Albuquerque	8.60
Seattle	15.43
Average	12.08
Std Dev	3.76791